

Submerged barrier evolution along the Mittag inner continental shelf, southern Namibia

By:

Marinja A. Bester

217004739

MSc Geology Dissertation
Supervisor: Prof. Andrew Green

College of Agriculture, Engineering and Science
School of Agriculture, Earth and Environmental Sciences
University of KwaZulu-Natal

Date: July 2024

Acknowledgements

I would first and foremost like to thank Jesus Christ. Although my faith may have wavered several times, He never did and the strength to complete this journey came entirely from Him.

I would like to express my sincerest gratitude to my supervisor, Prof. Andrew Green, for his consistent guidance and support throughout this study. His unwavering motivation, boundless patience and encouragement were crucial in helping me complete this dissertation. Despite the teary phone calls, his kind approach and concern for the well-being of his students is invaluable and is deeply appreciated.

I am grateful to have a supportive family who have written a few dissertations themselves and were able to give sound advice on how things should be and provide constructive criticism. I was instilled with a belief that I can accomplish anything I set my mind to and was always encouraged to chase my passions and work hard for them.

I would like to thank Lynette Kirkpatrick who is a strong role model as a leading female in the field. She is incredibly knowledgeable, approachable and was always willing to answer any questions and provide assistance where needed.

I would like to thank Tamera Heeralal for her unlimited moral, emotional and mental support as we braved our Master's together. Through countless late night work sessions, you helped me along throughout the whole process, be it with data, software, providing ideas or making hot chocolate to keep up the team morale. You are a friend I hold in the highest regard, and you have taught me so much, not only during this dissertation but life in general. I look forward to learning much more from you.

COLLEGE OF AGRICULTURE, ENGINEERING AND SCIENCE

Declaration 1 - Plagiarism

I, ……MARINJA BESTER……., declare that:

1. The research reported in this thesis, except where otherwise indicated, is my original research.

2. This thesis has not been submitted for any degree or examination at any other university.

3. This thesis does not contain other persons' data, pictures, graphs or other information, unless specifically acknowledged as being sourced from other persons.

4. This thesis does not contain other persons' writing, unless specifically acknowledged as being sourced from other researchers. Where other written sources have been quoted, then:

a. Their words have been re-written, but the general information attributed to them has been referenced

b. Where their exact words have been used, then their writing has been placed in italics and inside quotation marks and referenced.

5. This thesis does not contain text, graphics or tables copied and pasted from the Internet, unless specifically acknowledged, and the source being detailed in the thesis and in the References sections.

Student Signature 

.....

Supervisor Signature 

.....

Date: 18/07/2024

.....

Preface

The research described in this thesis was undertaken in the School of Geological Sciences (Marine Geology Research Unit), University of KwaZulu-Natal, under the supervision of Prof. A.N. Green. The duration of the work performed spans January 2021 to July 2024. These studies represent original work by the author and have not been submitted in any form to another university. Where use was made of the work of others, it has been duly acknowledged in the text.

Abstract

The inner continental shelf of southern Namibian coast hosts the world's largest diamond mega-placer deposit, which is intricately linked to the evolution of the Orange River and the formation of its submerged delta. The entrapment of diamonds is enhanced by the unique geological topography of the coast. Once such area where diamond prospecting is intended, the inner continental shelf offshore Mittag of southern Namibia, provides an opportunity to examine a series of submerged, and potentially diamond-rich, gravel shorelines. The inner shelf of Mittag comprises a Cretaceous siltstone basement seaward and Precambrian schist in the inner regions, overlain by enigmatic, and continuous coast parallel ridges observed in seismic reflection. These features span depths between -100 m and -55 m, showing composite, progradational, aggradational multistacked and retrogradational patterns. These features are characterised by an external peaked morphology and a channelled-high amplitude chaotic reflector internal geometry. Occasional landward directed moderate amplitude reflectors overlie the peaks and infill the channels. These are in turn overlain by low amplitude/acoustically transparent muds, with a prominent transgressive sandsheet along the inner shelf.

Cores reveal the unusual subcropping features to comprise gravels, interpreted as gravel-barriers and spits that formed during lower periods of sea level. The proposed evolutionary model demonstrates a complex interaction of sediment supply, sea-level changes, and bedrock control. Initial development created a broad sheltering lee in the bedrock, followed by gravel deposition during repeated regressions and transgressions, forming prograded barrier spits, downstepping barriers, and mixed sand-gravel shorefaces. Subsequent transgressions led to barrier rollover and back-barrier depression, forming extensive barrier spit-lagoon systems. The stratigraphy records stepped sea-level rises and emphasizes the significant role of

geological control in barrier system development and preservation. Given the erosional nature of this shelf, their preservation suggests links to rapid rates of sea-level rise (melt water pulses-MWPs). The rhythmic fluctuations of sea level during the Pleistocene have acted to create and preserve a series of barrier spit and back barrier environments on the shelf via normal regression and later overstepping of the barrier and back barrier complex. These barriers thus provide useful archives for sea level change from a far field site.

Table of Contents

Acknowledgements ii
Declaration 1 - Plagiarism iii
Preface iv
Abstract v
Chapter 1: Introduction 2
1.1 Context of Research 2
1.2 Aims and Objectives 3
Chapter 2: Literature Review 5
2.1 Regional Geology 5
2.2 Sediment Supply and Coastal Regime 7
2.3 Seismic stratigraphy: Classification and Reflector Patterns 10
2.4 Reflection termination patterns 11
Chapter 3: Methodology 14
3.1 Geophysical Data 14
3.1.1 Data Acquisition 13
3.1.2 Data Analysis 15
3.2 Lithostratigraphic Data 15
Chapter 4: Results 16
4.1 Seafloor geological and morphological framework 16
4.2. Seismic stratigraphy, lithostratigraphy and unit distribution 16
4.2.1 Acoustic basement and regional reflector SB1 19
4.2.2 WRS 20
4.2.3 Unit B: Basal fining up gravel 21
4.2.4 Unit C: Gravel with clay 22
4.2.5 Unit D: Sand 23
4.2.6 Unit E: Gravel 24
4.2.7 Unit F: Alternating clay and sand with clay as lowermost deposit 25
4.2.8 Unit G: Interbedded sand alternating with clay 25
4.2.9 Unit H: Interbedded sand and mud alternating with sand and clay 27
4.2.10 Unit I: Clay 27
4.2.11 Unit J: Fine sand and mud 27
Chapter 5: Discussion 32
5.1 SB1 32
5.2 Gravel barrier and shoreline environments 32

5.2.1 Unit B 32
5.2.2 Unit C 33
5.2.3 Unit D 35
5.2.4 Unit E 35
5.2.5 Unit G 35
5.3 Back barrier facies and environments 36
5.3.1 Unit F 36
5.3.2 Unit H and I 37
5.3.3 Wave ravinement surface (WRS) and post ravinement cover Unit J 37
5.4 The early shelf gravels: early to late Miocene pulses 37
5.5 The next generation: Late Pliocene to Pleistocene/Holocene pulses 38
5.6 Controls on beach emplacement and preservation 38
Chapter 6: Conclusion 42
References 44

Chapter 1: Introduction

1.1 Context of Research

The southern Namibian coast is host to the world's largest diamond mega-placer deposit, related to the evolution of the Orange River and the development of the diamondiferous Orange River submerged delta. The best established and most complex diamond placers can be found in the Sperrgebiet (the "Forbidden Zone") (Fig. 1.1) that extends northward up the coast from Oranjemund to Lüderitz, in which substantial diamonds, closely associated with gravels and palaeo-shorelines, are found. However, diamonds are not just located along the coastline, but are found offshore in significant quantities and with high grades (Runds, 2018).

The Orange River erodes the diamonds from central South Africa over the kimberlite-rich Kaapvaal craton (Garnett, 2017), and transports them to the wave-dominated, micro-tidal west coast of South Africa and Namibia (Jacob, 2001; Runds, 2018). Through transportation, the diamonds are rounded and polished by collision with other particles also in transport, thus making the west-coast a highly sought-after region in terms of coastal and marine diamond mining. The diamonds are further distributed northward along the coast by the vigorous longshore drift regime, and southward by the southward dominating surface winds (De Decker, 1988). To the north and with increasing distance from the Orange River, gravel accumulation and diamond size decreases as the heaviest deposits are naturally dropped closest to point of discharge on the coast (Apollus, 1995; Hallam, 1964; Spaggiari et al., 2006).

Offshore, the mining of diamonds has steadily increased as the early technical challenges have been overcome with increasingly sophisticated exploration, surveying and mining techniques. The seabed is thus the new frontier for mining, especially on the inner shelf adjacent to areas

of significant gravel quantities and diamond resources (Kirkpatrick and Green, 2021). Located on the south-western coast of Namibia ~ 45 km north of the Orange River mouth, the Mittag continental shelf extends seaward of active mining areas and is bordered on either side by submerged gravel barrier deposits preserved in the stratigraphy (Kirkpatrick et al., 2019; Runds et al., 2019). The shelf thus has potential for the preservation of gravelly submerged shorelines on which this dissertation focuses.

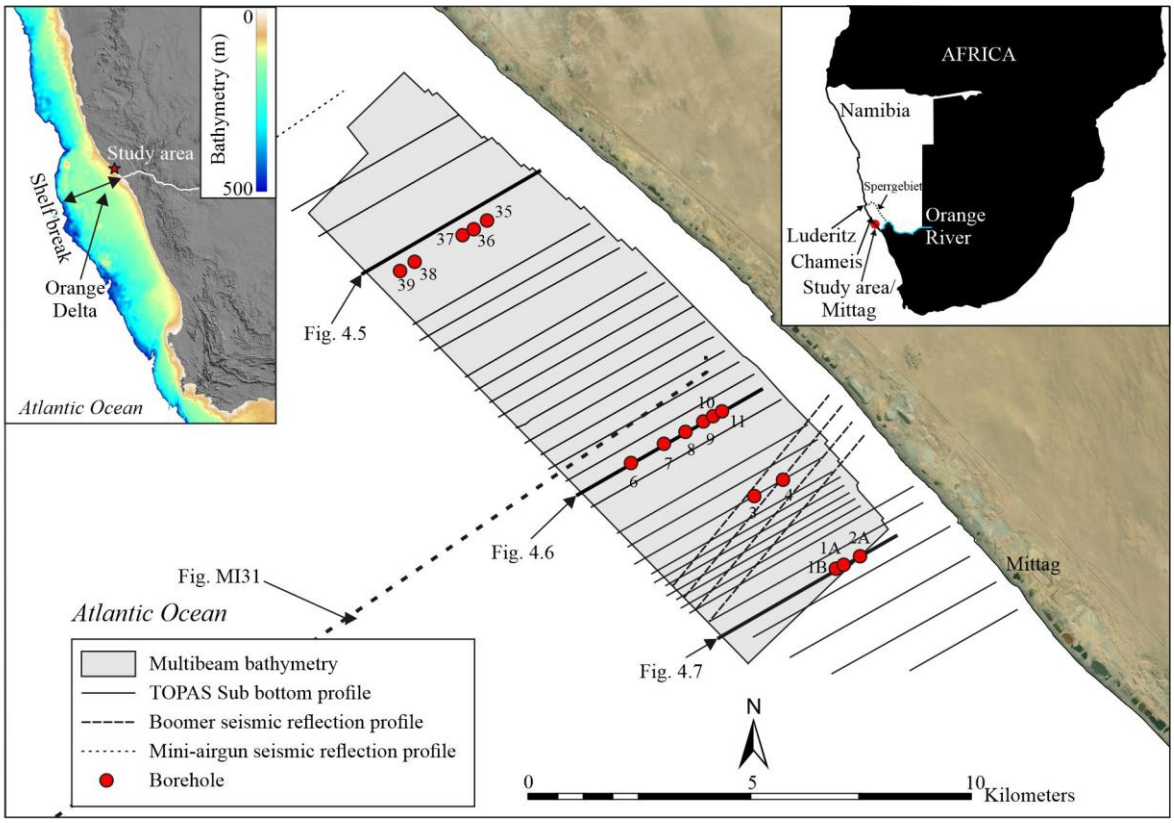


Figure 1.1: Study area locality map. The distribution of the data is outlined, in addition to the key figures presented in text. Upper left inset depicts study area in relation to the regional bathymetry of the shelf and outlines the Orange River and associated Orange Delta.

1.2 Aims and Objectives

This dissertation aims to examine the distribution, structure and evolution of submerged gravel deposits over an 80 km^2 portion of the Mittag inner continental shelf of southern Namibia.

Objectives include:

1) to examine the seabed and subsurface structure and morphology of the bedrock

2) to produce a seismic stratigraphy of the unconsolidated sediment units.

2) to correlate seismic units to lithological data obtained from of boreholes.

3) to interpret in detail, the shelf's palaeo-depositional environments.

4) to provide a model for the development and preservation of the various submerged gravel shoreline features in the study area.

Chapter 2: Literature Review

2.1 Regional Geology

The west coast of southern Africa comprises a passive continental margin (Fouché et al., 1992), the result of the break-up of Gondwana in the Early Cretaceous (Runds et al., 2019) and was characterised as such by the tectonic stability that followed a stage of intracontinental rifting and breakup (Braun and Beaumont, 1989; Lister et al., 1991). Approximately 120 million (Ma) years ago, the formation and assembly of the present-day morphology and stratigraphy of the shelf began, with rifting that eventually separated the South American plate and the African plate, forming the South Atlantic Ocean (Lovecchio et al., 2020), and consequently the Orange Basin (Dingle, 1992; Kuhlmann et al., 2010). Rabinowitz and LaBreque (1979) considered this process diachronous, initiating from the south and gradually propagating northwards (Rabinowitz and LaBrecque, 1979). The gradual northward ocean spreading was accompanied by magmatic activity (Lovecchio et al., 2020). According to Kuhlmann et al. (2010), the syn-rift phase of ocean spreading was manifested as a series of north-south trending grabens and half-grabens, predominantly comprising volcanic successions staggered along the continental margin. These half grabens preserve rocks aged between Late Carboniferous to Early Jurassic (potentially the Karoo Supergroup).

The formation of the Orange Basin related to two main tectonic events; a Late Jurassic to Lower Cretaceous syn-rift mega sequence and a Cretaceous to present-day post-rift mega sequence (De Vera et al., 2010). These two events are separated by a Late Hauterivian unconformity of 130 Ma (De Vera et al., 2010; Hirsch et al., 2010). Progressive filling of the available accommodation during the drift phase of margin development followed with Cretaceous to Early Tertiary strata deposited on the proto shelf. These formed a seaward-thickening wedge

of sediment that rests atop an angular unconformity (Stevenson and McMillan, 2004). These Barremian to Cenozoic deposits are termed the "Orange River Delta" succession (Stevenson and McMillan, 2004). Cretaceous to Cenozoic-age deposits mainly consist of Neogene limestones, mudstones and siltstones of varying degrees of competence (Compton and Bergh, 2016; Rogers, 1977). The Uppermost Quaternary sediment forms a thin unit ~ 1 m thick unit that covers the entire Namibian continental shelf. It thickens locally to about 40 m on the inner shelf, middle shelf and to the outer shelf slopes (Stevenson and McMillan, 2004).

During the steady filling of the Orange Basin, deposition was punctuated by periods of uplift during the Upper Cretaceous (Late Campanian), associated with a phase of hinterland uplift (Guillocheau et al., 2012) (Fig. 2.1 a), with a further two periods of uplift (Lower Palaeocene and the Middle Oligocene) identified by Siesser and Dingle (1981). A final late Oligocene unconformity, formed by a less prominent phase of uplift (Baby et al., 2018), formed minor unconformities in the delta (Guillocheau et al., 2012).

The margin physiography reflects the above effects of uplift, namely in a stepped topographic profile, with four distinct morphological regions from the coast to seaward. The shallow areas are characterised by a rocky nearshore platform to ~30 m depth, with the inner shelf extending to ~ -130 m where a wave-cut terrace marks the lowstand shoreline of the Pleistocene glacial maxima (Rogers, 1977). The outer shelf is a gently sloping feature (<1°), extending from depths of 200 m to 500 m (Rogers, 1977; Rogers and Rau, 2006). This deepens gradually from the indistinct shelf break to the continental slope (Rogers, 1977).

This study focuses on the inner shelf, so particular attention will be focused on this morphological domain. The inner shelf is marked by a step-like bedrock morphology, often

expressed in the bathymetry where sediment cover is scarce, interpreted to represent wave-cut platforms and cliffs formed during sea-level still-stands (Hallam, 1964; Jacob et al., 2006; Kirkpatrick and Green, 2021; Murray et al., 1970). These have been cut into siliciclastic/metamorphic rocks of the Oranjemund Formation (Jacob et al., 2006; Kirkpatrick and Green, 2018), which crop out along the innermost portions of the shelf. To north and south, much of the inner continental shelf's step-like morphology is concealed by a thick unit of soft sediment and mud deposited during the Holocene period after the Last Glacial Maximum (LGM) (Green et al., 2024).

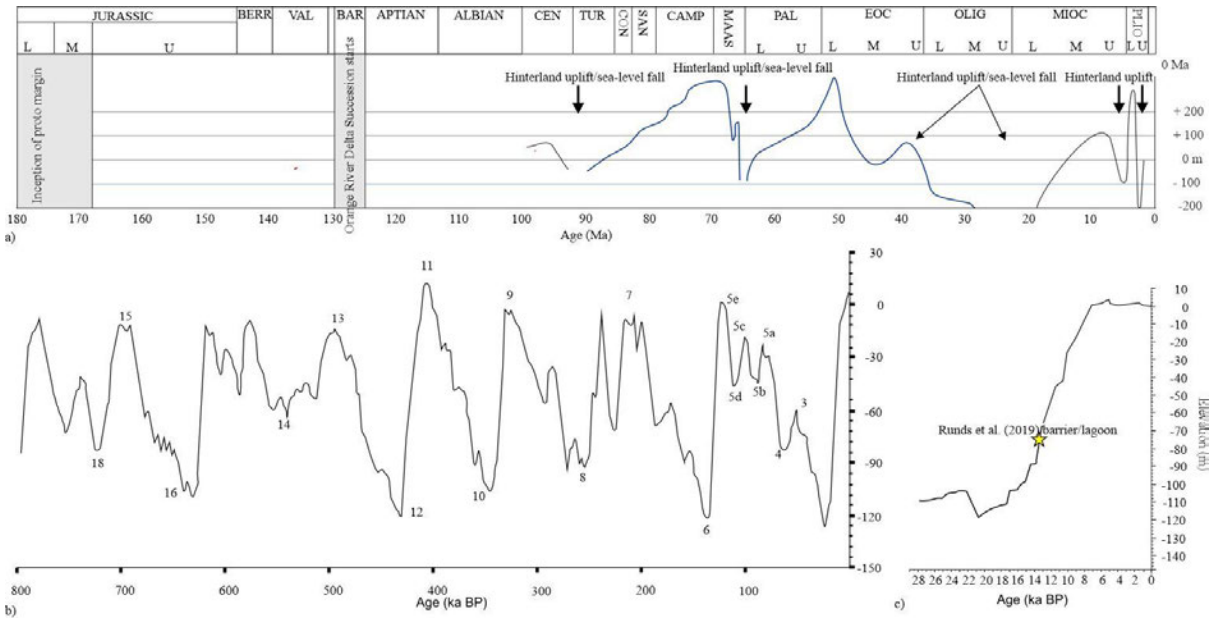


Figure 2.1: a) Regional sea level curves compiled from Siesser and Dingle (1981), b) Pleistocene sea level stack from Spratt and Lisieki (2016) and c) Late Pleistocene to Holocene sea level curve of Cooper et al. (2018). (Modified after Green et al., 2024).

2.2 Sediment Supply and Coastal Regime

The Orange River, which acts as the principal conduit of sediment to the west coast of southern Africa, was established during the Early Cretaceous (Dingle and Scrutton, 1974). Since this time, the west coast of Namibia has been considered to operate as an upper micro-tidal to meso-tidal, wave-dominated coastline (Kirkpatrick et al., 2019). In wave-dominated settings along the coastline, much of the delta lies submerged and the nearshore portions form diminished features subject to reworking and transport by longshore currents (Kirkpatrick et al., 2019).

Sediment transport along the shelf and margin varies (Fig. 2.2). The Orange River presently delivers a less voluminous and now finer-grained load to the inner shelf than previously (Bluck et al., 2007; Hoyt et al., 1969). This comprises fine gravel, sand, silt, and clay (Bluck et al., 2007), as compared to boulder sized sediments during the Late Cenozoic. The finer components are entrained in the littoral zone for several thousand kilometres, being traceable into southern Angola (Garzanti et al., 2018).

The coarser materials are concentrated along the southern Namibian coast and shelf up to Chameis Bay (Runds et al., 2019; Spaggiari et al., 2006), ~ 65 km north of the study area. Sand is retained in the nearshore and transported along the coast in a northerly fashion by a vigorous longshore drift driven by consistently high wave energy and oblique approach angle (Bluck et al., 2007; Bluck et al., 2001). These have prevailed since the middle to late Cenozoic (Bluck et al., 2007; Spaggiari et al., 2006). At coastal inflection points, sand is returned onshore to contribute to the main Namib Desert Sand Sea (Bluck et al., 2007; Lancaster and Ollier, 1983), exacerbated by the rocky outcrop and lack of accommodation in the nearshore (Green et al., 2024).

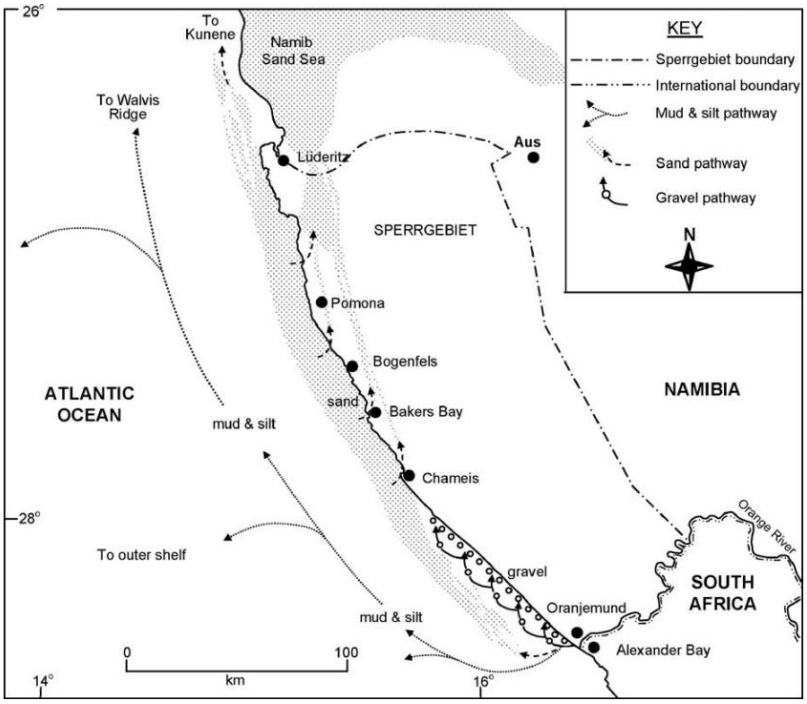


Figure 2.2: Map showing the sediment dispersal paths of gravel, sand and mud northward along the high energy Namibian coastline (Spaggiari et al., 2006).

The terrigenous mud fraction (most notably supplied by the Orange River), is transported mostly as a mobile nepheloid layer to form an up to 15-m-thick Holocene-age mud belt on the inner to mid shelf (Bremner and Willis, 1993). The contemporary shelf bathymetry, inshore of the gradient knickpoint of the inner shelf break provides accommodation not just for the mudbelt, but for other significant depocenters (Runds et al., 2019) (Fig. 2.3).

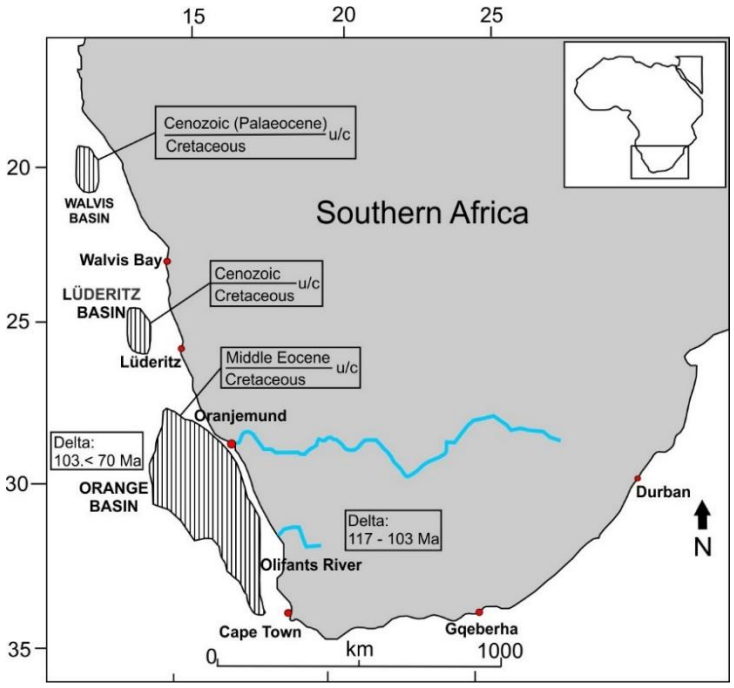


Figure 2.3: *The Orange River and associated shifts in depocenter over time and space. Modified from Bluck et al., (2007).*

2.3 Seismic stratigraphy: Classification and Reflector Patterns

The study of the depositional patterns by acoustic means, developed and modified by changes in sediment supply, accommodation and prevailing energy regime, is termed seismostratigraphic analysis (Roksandić, 1978; Veeken and Van Moerkerken, 2013). This can be best described as the investigation, by seismic reflection profiling (or sub bottom profiling) of the reflections in individual packages, bound by major reflections or unconformity surfaces, known as seismic facies (Veeken and Van Moerkerken, 2013). The differentiations between the reflection characteristics are due to the reaction of the different facies with the acoustic pulses released during acquisition of seismic or sub bottom data. The term “facies” is mainly used to denote the differences in acoustic appearance based on the composition and biologic content between different lithostratigraphic units (Roksandić, 1978). This can be used to separate certain seismic facies based on their unconformity boundaries and the acoustic reflection characteristics like their internal reflection amplitudes, continuity and configuration

and frequency contents, which can all be collected and analysed. The interactions change and vary based on the nature of the unit, including the physical properties of rocks or sediments (Veeken and Van Moerkerken, 2013).

According to Veeken and van Moerkerken (2013), the information about the depositional environment of the seismic facies is encapsulated in the following internal reflection descriptions: prograding, aggrading, convergent, divergent, chaotic, parallel, subparallel, sigmoid, oblique, hummocky, wavy and reflection-free (Mitchum Jr et al., 1977; Roksandić, 1978; Veeken and Van Moerkerken, 2013) (see Fig. 2.4 below). To correctly classify these seismic facies and internal reflections, a seismic facies analysis index system was proposed, which includes detailed accounts of the nine independent parameters: position, external form, internal configuration, continuity, smoothness, amplitude, frequency, special waveforms and appearance (Roksandić, 1978; Sheriff, 1976; Xu and Haq, 2022).

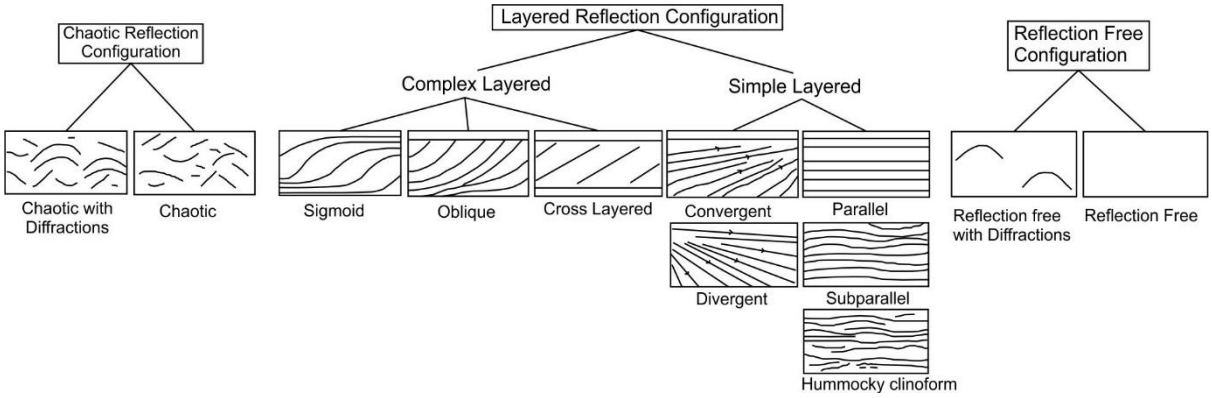


Figure 2.4: Diagram showing the different types of internal reflector configurations. Modified from Roksandić (1978) and Mitchum et al., (1977). Reflection free is often termed acoustically transparent.

2.4 Reflection termination patterns

With sea-level fluctuation, changing energy regimes, shifts in material type and sediment discharge, and changes in erosion, seismic reflections will present certain termination indicators to represent these changes. Reflection terminations as described by Catuneanu

(2006), are interpreted as geometric relationships between the strata and the stratigraphic surface they terminate onto (Catuneanu, 2006). It is by these unconformities or correlative conformities at the top and base that facies units can be identified and interpreted, thus allowing one to interpret the depositional sequence (Mitchum Jr et al., 1977).

Chronostratigraphically, depositional sequences were deposited during an interval of geologic time limited by age of boundaries where the boundaries are conformities; however, where the boundaries are unconformities, the age ranges of the strata within the sequence can differ immensely from place to place. This is due to a hiatus that took place, a passing of time or lost time. Conformable boundaries are not measurable in time and are believed to be synchronous, not the case in unconformities (Mitchum Jr et al., 1977). Unconformities are best identified based on their discordant relation, indicating whether they result from erosion or nondeposition (Catuneanu, 2006). Nondepositional hiatuses are indicated by onlap, downlap and toplap (Fig. 2.5), whereas truncation represents an erosional hiatus as the result of structural disruption (Mitchum Jr et al., 1977; Mitchum Jr et al., 1977).

In combining the internal reflection facies and external reflector characteristics, inferences can thus be made on the state of sea level, the nature of material and its relative contribution to available accommodation space, in addition to the depositing environments and mechanisms (Veeken and Van Moerkerken, 2013). These are in turn balanced with reference to other works, where groundtruthing has been carried out, or to available groundtruth data. As such, lithostratigraphy may be linked to the seismic stratigraphy to produce a broad scale, spatially robust geological model.

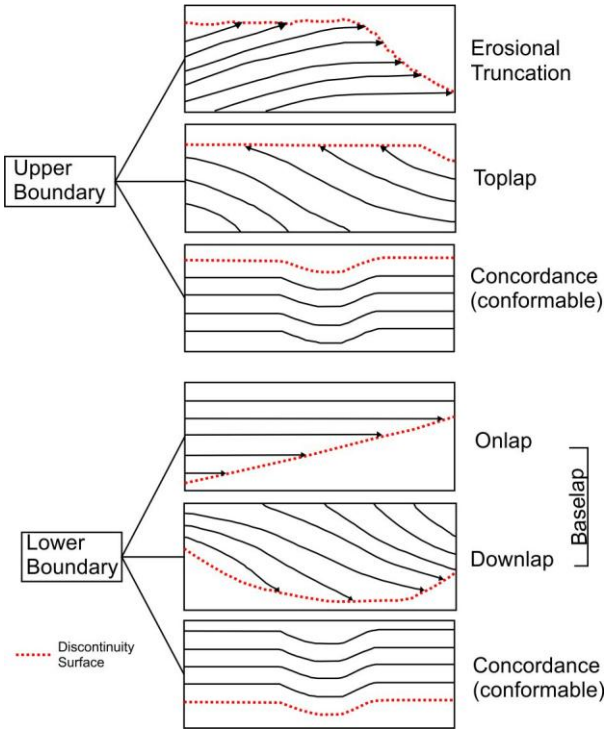


Figure 2.5: Diagram showing the various termination patterns on the upper and lower boundary units by conformities or unconformities. Modified from (Mitchum Jr et al., 1977).

Chapter 3: Methodology

3.1 Geophysical Data

3.1.1 Data Acquisition

Several different tools were employed for the examination of the study area's substrate. A regional survey to outline the broad stratigraphy was conducted using a 6-inch mini airgun with a 24-element streamer. The data were bandpass filtered from 500 to 1200kHZ, bottom tracked, deconvolved and swell filtered. These data show the shelf to slope stratigraphy with a vertical resolution of ~ 1 m.

A Kongsberg Topas PS40 parametric sub-bottom profiler was used to collect a dense grid of sub bottom profiles over the study site for outlining the sub-bottom in ultra-high resolution. The system employed a ricker pulse using a pulse interval of 500 ms. The data were converted to .segy format, then band pass filtered between 1000 and 8000 Hz, bottom tracked, swell filtered and supplemented with time varied gains in Geosuite Allworks. The vertical resolution of the data is ~ 20-30 cm.

Deeper penetration seismic reflection data, outlined by Kirkpatrick and Green (2017), were collected using a Geoacoustics 175 J Boomer system coupled with a towed 18-element hydrophone array. The data were collected using a CODA DA4G system. These data overlapped a portion of the southern area offshore Mittag and we thus included to provide a broader area of scope. Once collected, the segy data were imported into Geosuite Allworks where they were band pass filtered between 300 and 3000 Hz, bottom tracked and swell filtered. The data resolve in the vertical domain to ~ 75 cm.

In order to examine seafloor morphology, bathymetry was collected using a Reson Seabat 8111 multibeam echosounder (MBES), with a TSS DMS-05 (Dynamic Motion Sensor) as the motion reference unit. The data were reduced from soundings using tide tables provided by the navy and several sound velocity casts. These data were processed using the Hypack utility and the final charts exported as a 1 x 1 m grid relative to Mean Sea Level (MSL).

3.1.2 Data Analysis

The sub bottom profile data were all interpreted in Geosuite Allworks, where the major unit bounding unconformities were digitised. The data were converted from travel time to depth in meters using a standard sound velocity of 1500 ms^{-1} in water, and 1650 ms^{-1} in sediment. Isopach files for each unit were exported for gridding in Golden Software Surfer v. 12 using the Kriging technique.

3.2 Lithostratigraphic Data

To supplement the geophysical data, several cores were collected using the M/V The Explorer. equipped with a reverse-circulation (RC) drill capable of retrieving samples up to 8 m deep. Material that entered the rotating drill apertures (170 × 170 mm) at the seabed was logged with the screening of coarser (maximum diameter > 19 mm) and finer (maximum diameter < 1.5 mm) clast sediments in sample bins whenever a change in lithology was observed with depth. The clasts were visually assessed on the basis of grain size, composition and textural characteristics (Tucker, 1988). Photographs were taken of each individual sample screen**.** A total of 15 holes were drilled of varying depths and sampled for lithostratigraphic analysis and

radiocarbon dating. The lithostratigraphy was correlated with individual sub bottom profiles using the wells function in GeoSuite Allworks.

Chapter 4: Results

4.1 Seafloor geological and morphological framework

The proximal inner shelf of the study area is dominated by high relief outcrop of Proterozoic schists and phyllites that comprise the coastal bedrock. These form a rugged nearshore topography (Fig. 4.1). Superimposed along the seaward edge of the bedrock are outcrops of silcrete that create a distinctive pinnacled and highly irregular seafloor; together bedrock and silcrete form the geological framework for the inner shelf and shoreface.

To seaward and at a depth of ~ 45 m, the bedrock and silcrete transition to smooth, featureless seafloor with isolated sorted bedforms. A 2.7 km-wide corridor of sediment transects the bedrock in the centre of the study area forming a smooth and featureless coast perpendicular channel (Fig. 4.1).

4.2. Seismic stratigraphy, lithostratigraphy and unit distribution

A total of ten seismic units (B-J) and two regional seismic reflectors (SB1 and WRS) (Fig. 4.2-4.7) were identified from the sub bottom data (Table 4.1). All units were defined on the basis of their individual characteristics such as internal reflection configurations, reflection amplitudes, termination patterns, bounding reflectors, and reflector continuity. The spatial distribution and thicknesses of each unit are presented in Figure 4.2. Figure 4.8 outlines the lithostratigraphy of the various units.

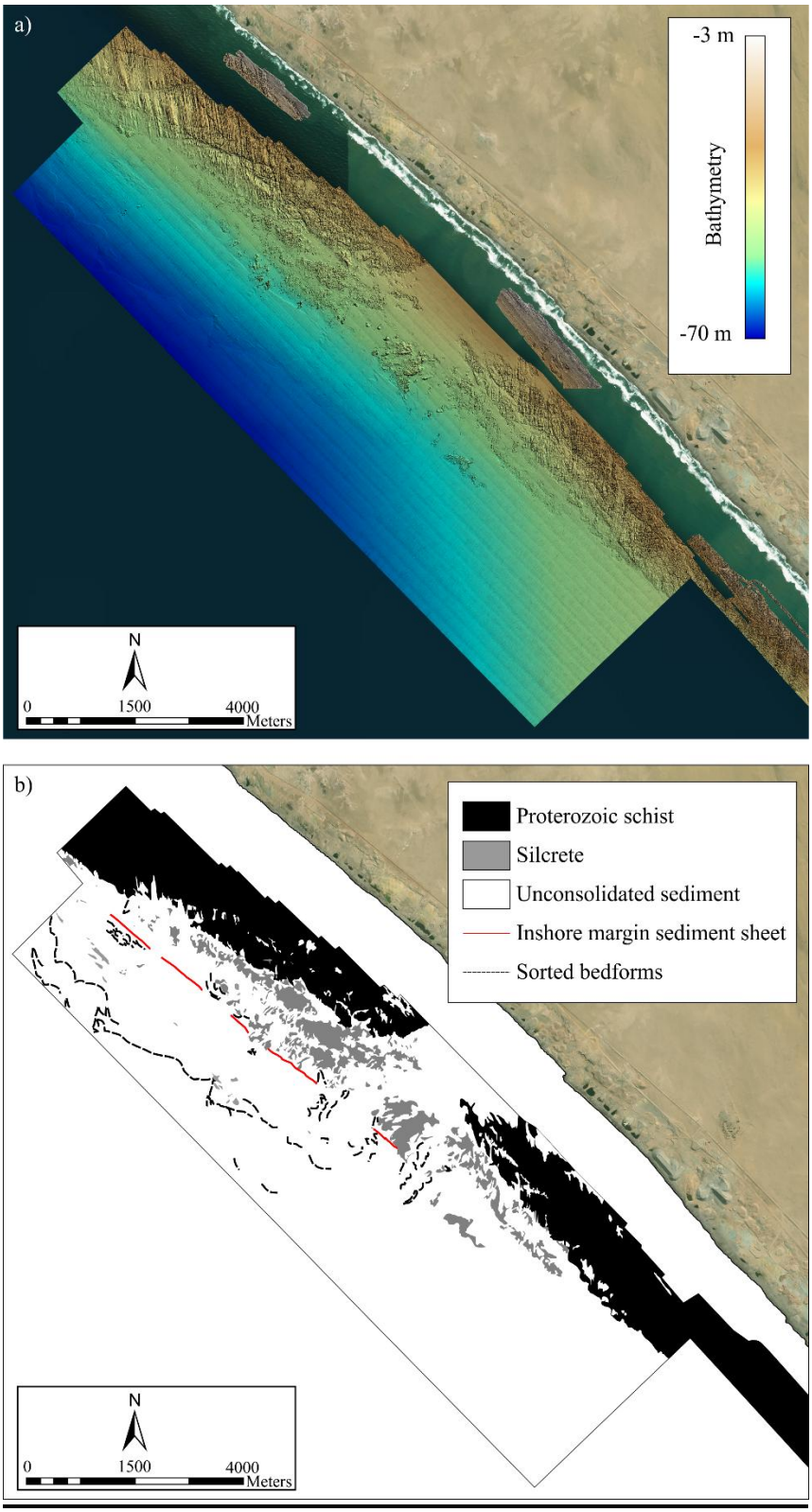


Figure 4.1: Images of the study area. a) Multibeam bathymetry of the seafloor indicating depth variations, b) seafloor interpretation of bedrock composition, namely schist, silcrete and unconsolidated sediment.

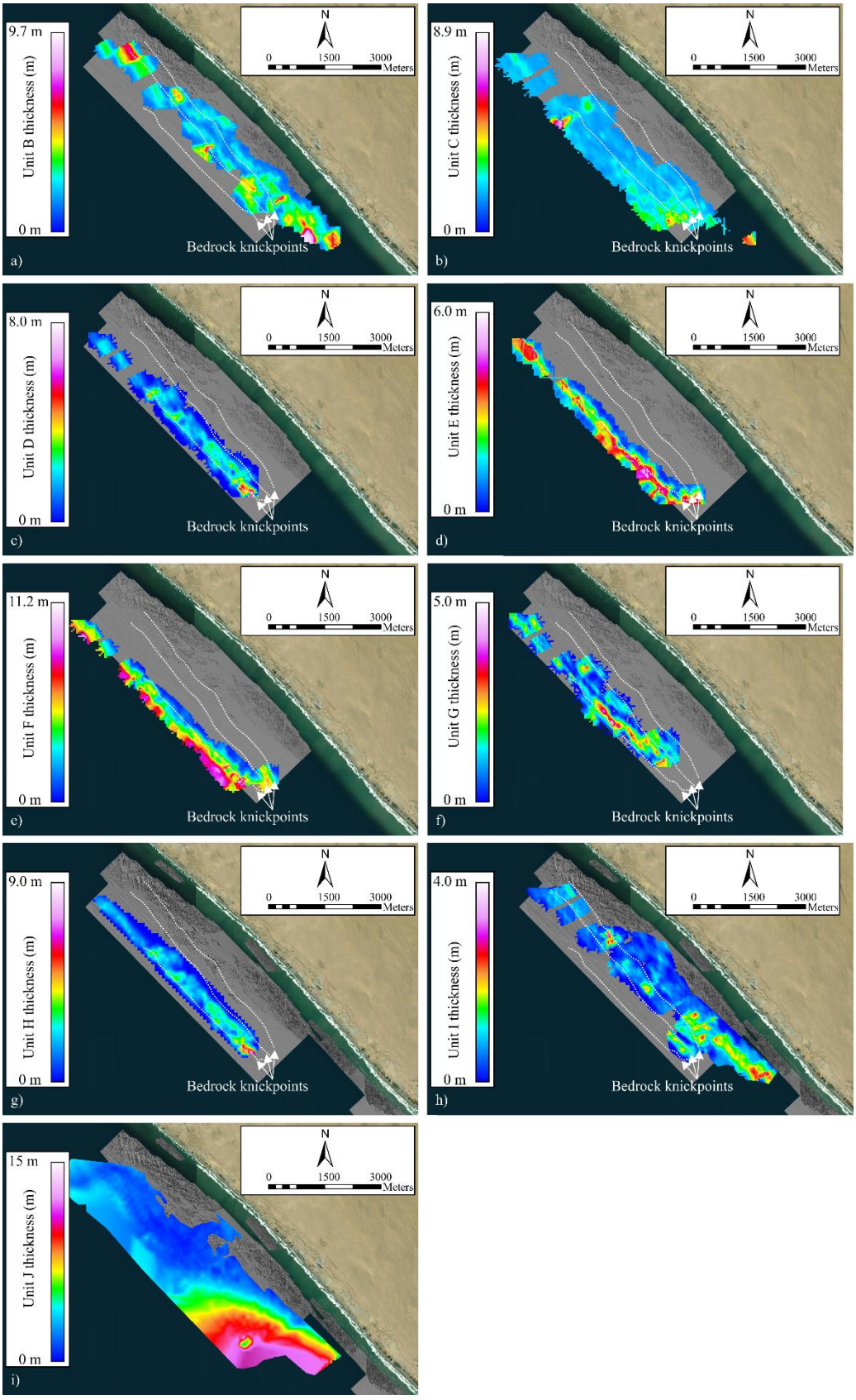


Figure 4.2: Isopach maps for the various seismic and lithostratigraphic units. a) Unit B (basal fining up gravel), b) Unit C (gravel with clay), c) Unit D (sand), d) Unit E (gravel), e) Unit F (alternating clay and sand), f) Unit G (interbedded sand alternating with clay), g) Unit H (interbedded sand and mud alternating with sand and clay), h) Unit I (clay), i) Unit J (fine sand and mud).

4.2.1 Acoustic basement and regional reflector SB1

The acoustic basement (Unit A) is marked by two key seismic packages. Inshore the acoustic basement comprises acoustically chaotic, high amplitude internal reflections, with irregular hyperbolic diffractions (Fig. 4.3). To seaward these are onlapped by prograding, moderate to high amplitude, high continuity seaward dipping reflections. Together these represent the inshore Proterozoic bedrock and onlapping Cretaceous siltstones identified by Kirkpatrick et al. (2019).

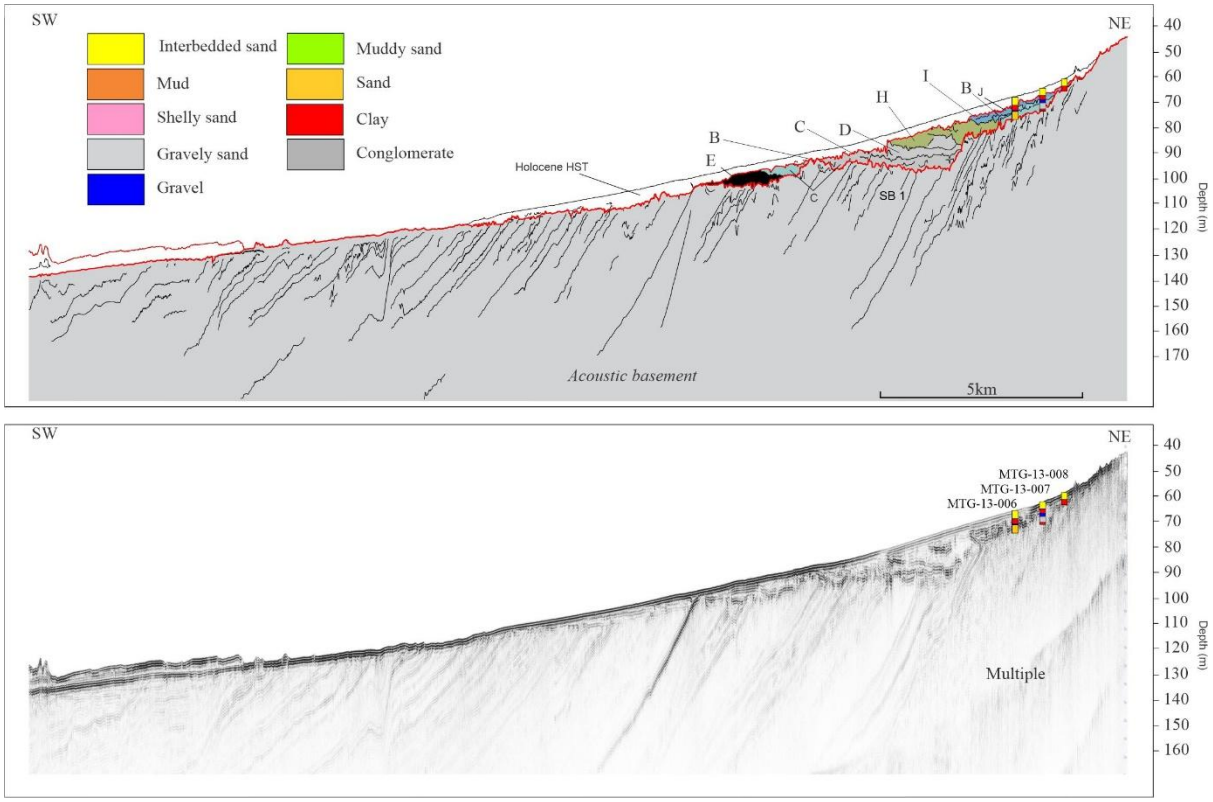


Figure 4.3: (Above) Mini airgun seismic line displaying a regional depiction of the geology of the continental shelf with interpretations of the sedimentary units and (below) the processed seismic line.

The acoustic basement is truncated by the SB1 regional reflector, separating the Proterozoic basement unit (Unit A) from the unconsolidated upper units. SB1 forms a seaward-dipping, irregular surface with three knickpoints forming terraces at -78 msl, -65 msl and -55 msl (Fig. 4.4 a). The terraces have a slope of ~ 0.2° and a steepened bedrock profile of ~ 0.7° (Fig. 4.4

b). The deepest terrace fronts a comparatively steeper area of bedrock of ~1° (Figs. 4.4 a and b).

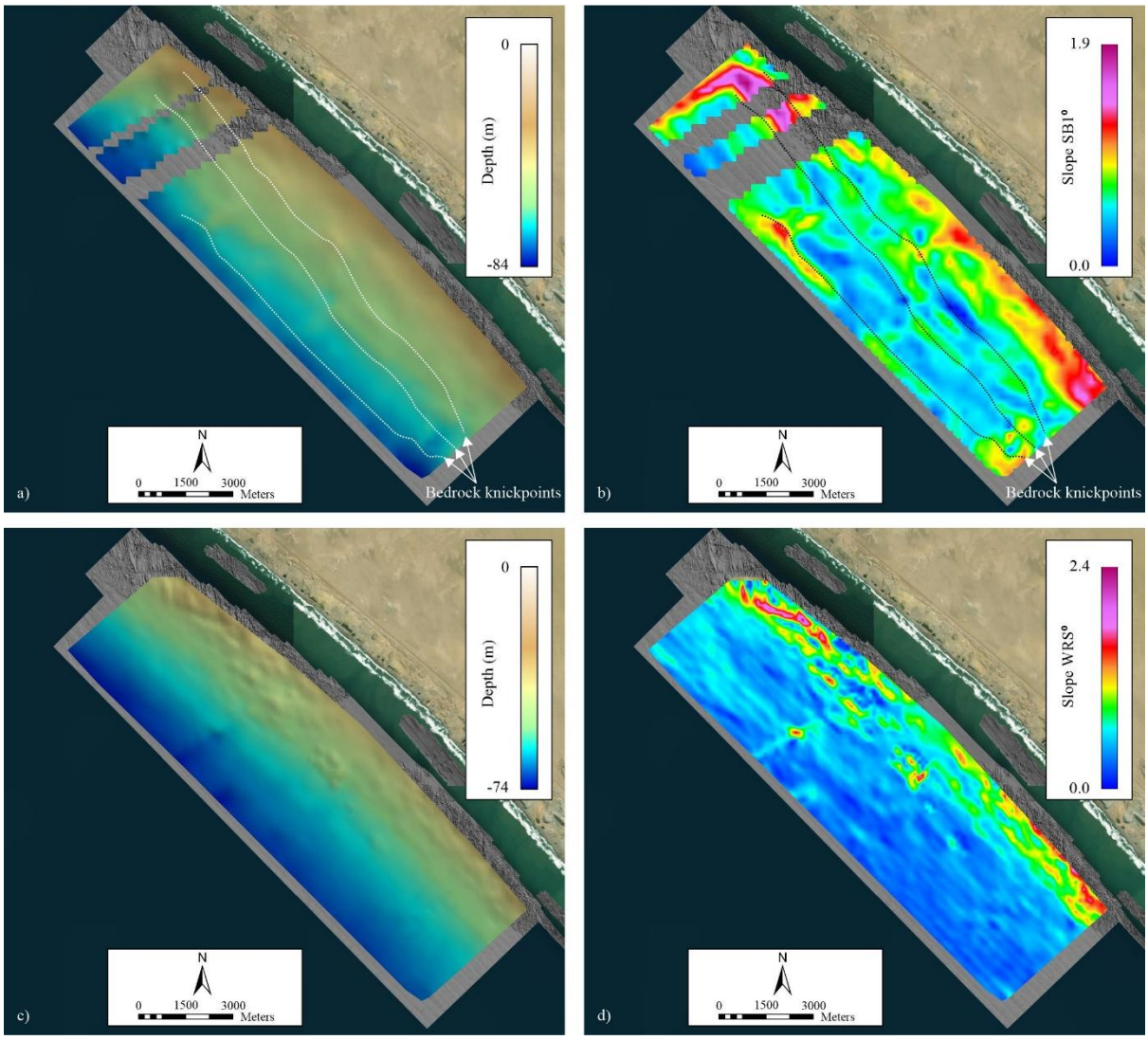


Figure 4.4: Surfaces of the study area representing various focuses. a) surface of SB1 with the knickpoints in the bedrock at -78 msl, -65 msl and -55 msl. b) surface of SB1 depicted in terms of slope angle with the three knickpoints. c) surface of the wave ravinement surface (WRS) with regards to depth. d) surface showing the slope angle of the WRS.

4.2.2 WRS

WRS forms a relatively gently seaward dipping erosional surface (average 0.4°) that truncates the underlying stratigraphy and merges with SB1 where bedrock crops out along the innermost shelf. These areas are marked by topographic irregularities in the surface profiles (Fig. 4.4 c). This trend is reflected in the local increases in surface gradient from 1° to 2.4° in the nearshore

(Fig. 4.4 d). Isolated points where gradient increases in the more seaward portions of the study area are marked by rises in the topography of SB1 (Fig. 4.4 d).

4.2.3 Unit B: Basal fining up gravel

Unit B is situated at - 45 to - 60 m and is arranged in a backstepping fashion. Its seismic facies comprise low amplitude, sub-parallel, wavy and relatively flat lying internal reflections. In some areas the reflectors appear to be irregular and chaotic (Fig. 4.5). Unit B forms two linear, coast-parallel bodies which vary in thickness along strike, in some cases constrained by bedrock high points (Fig. 4.5; Fig 4.2 b). Cores reveal the unit to comprise large well-rounded cobbles of sandstone and quartz-rich breccia were confined by bedrock. In the more open areas, this comprises cobbles mixed with reworked pebbles of saprolite (Fig. 4.8 a, c and f) that fine up into sands with increasing shelly content (Fig. 4.5). The unit forms mounds where the internal reflection geometry is aggradational and marked by irregular to wavy high amplitude reflections. These reflections downlap SB1.

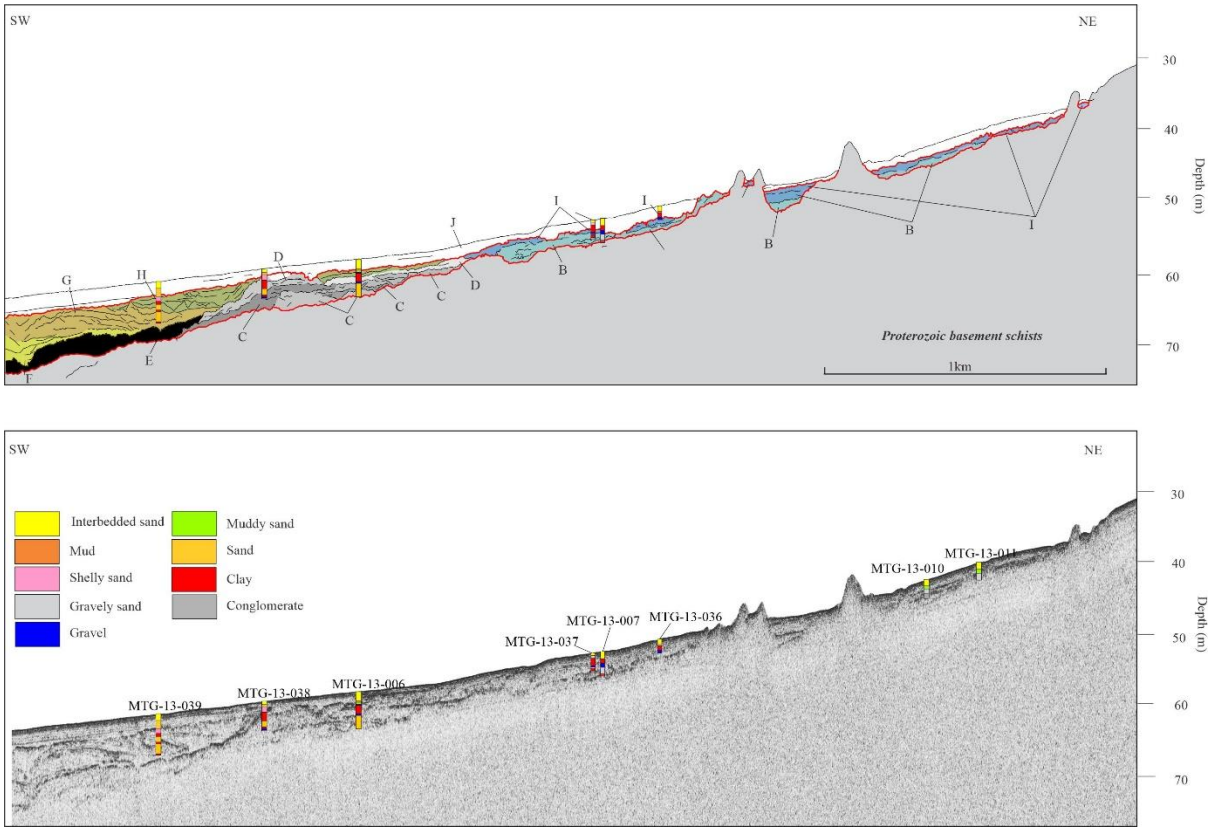


Figure 4.5: (Above) Interpreted to show Very high-resolution, coast perpendicular TOPAS sub-bottom profile of seismic line number 6868378_060_TPS; (Below) The processed seismic line showing the drilled cores and their compositions. This line is present in the northern section of the study area.

4.2.4 Unit C: Gravel with clay

Unit C varies significantly in thickness (Fig. 4.2 b) and external morphology. In the north-west, Unit C has a relatively flat lying profile with a rugged lower boundary as it overlies and downlaps Unit B (Figs. 4.5, 4.6, 4.7). In the south-east, Unit C has a mound-like profile with short, discontinuous reflections and a chaotic and irregular high amplitude internal reflection configuration. Though evenly distributed at ~ 1 m thickness throughout the study area between depths of 70 to 65 m, two areas of increased thickness of up to ~ 8 m occur (Fig. 4.2 b). These correspond with abrupt increases in the bedrock gradient. Cores reveal the unit comprises well-rounded gravel ranging in size from approximately 2.5 cm to about 8 cm (Fig 4.8 b and d), with occasional layers of light grey clay varying in thickness forming bright internal reflections

(Fig.4.5). Minor exotic clasts appear in the gravel pebbles such as jasper and agate. The clay is found further offshore in the unit, with landward side of the unit having minimal clay present.

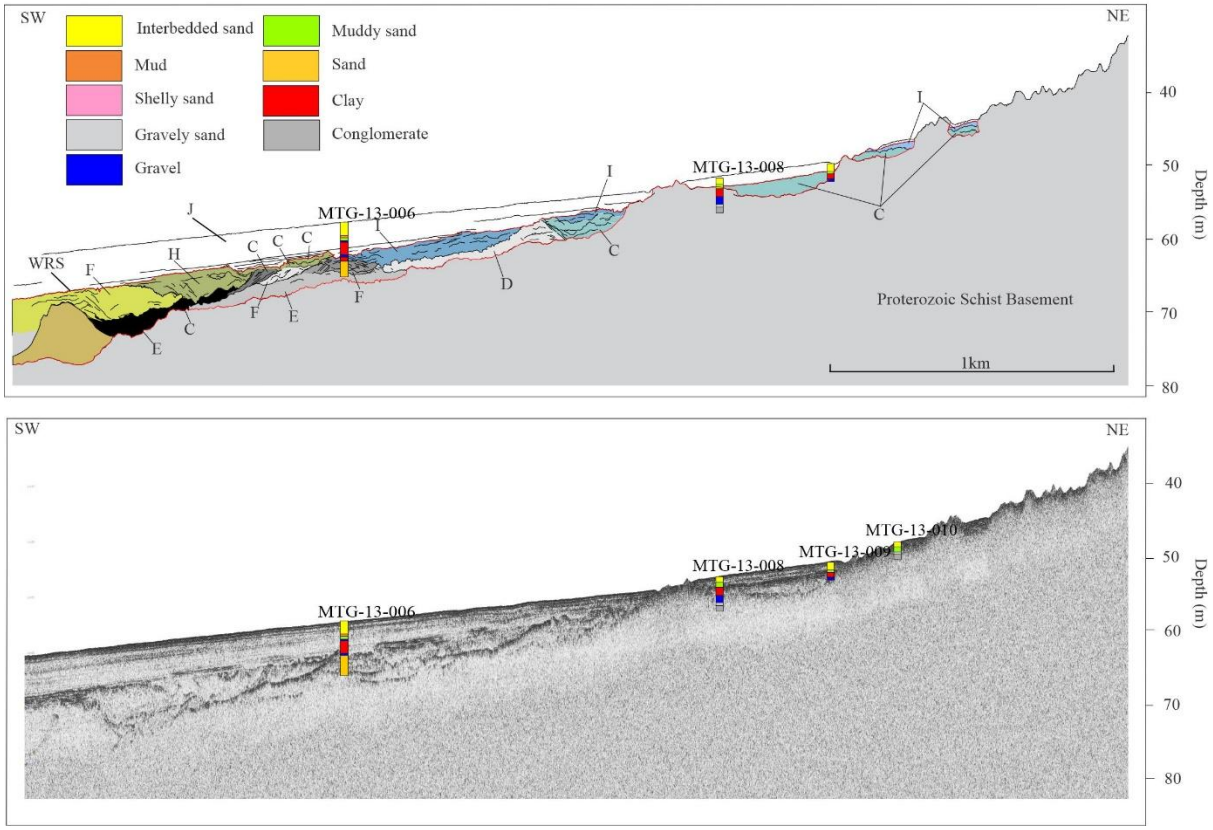


Figure 4.6: (Above) High-resolution, coast perpendicular TOPAS sub-bottom profile of seismic line number 6866900_060_TPS interpreted to show the identified sedimentary units; (Below) The processed seismic line showing the drilled cores and their compositions. This line is approximately present in the middle section of the study area.

4.2.5 Unit D: Sand

Unit D is an aggrading, prograding unit that rests atop Unit C (Fig. 4.5; 4.6) and either entirely progrades over, or onlaps it to seaward, from depths of 55 to 70 m (Fig. 4.7). Where it rests on Unit C, Unit D has a flat lying to mounded profile. However, where it has onlapped Unit C, it forms a wedge shape with clear prograding internal reflections. Figure 4.6 demonstrates the variability in the internal reflection configuration of the unit, with inclined seaward prograding

high amplitude reflections to the west of the mound, and landward, more shallowly dipping reflections to the east.

Unit D forms a NW-SE orientated linear feature of varying thickness along strike (Fig. 4.2 c), with maxima of up to 8 m. The unit consists of sand, notably in the mounded examples (Fig. 4.6).

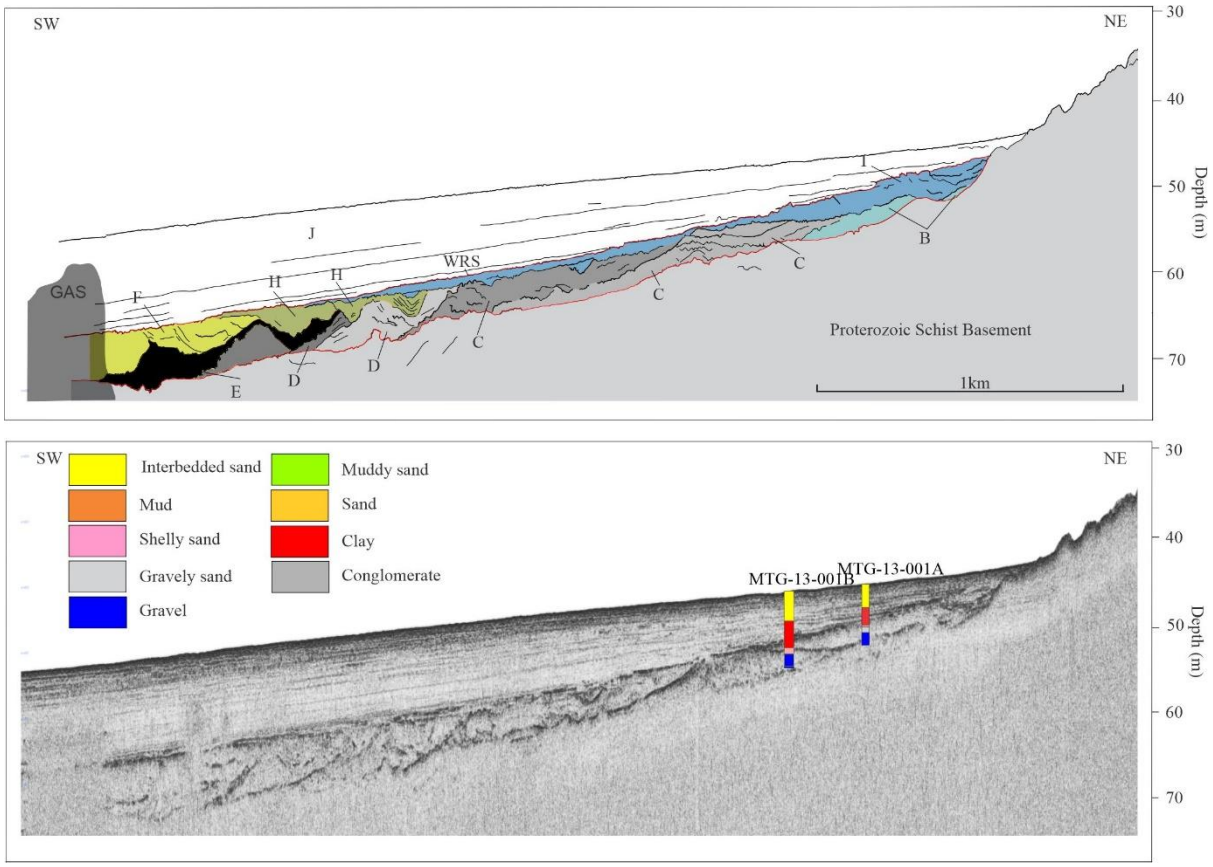


Figure 4.7: (Above) High-resolution, coast perpendicular TOPAS sub-bottom profile of seismic line number 6864536_060_TPS interpreted to show the identified sedimentary units; (Below) The processed seismic line showing the drilled cores and their compositions. This line is present in the southern section of the study area.

4.2.6 Unit E: Gravel

Unit E is marked by an acoustically opaque package that mantles SB1 and is bounded at its top by a high amplitude reflector (Figs. 4.5; 4.6; 4.7). It occurs at a depth of - 70 m and may occasionally form in low points within SB1 (Fig. 4.6). Unit E forms a linear body of sediment

that trends NW-SE and is approximately 600 m-wide and up to 6 m thick. The unit rests seaward of the prominent increase in the bedrock surface slope at -75 m (Fig. 4.4 a). The unit comprises sand with thin layers of well-rounded pebbles approximately 2 cm in size, including exotic clasts of jasper and agate (Fig. 4.8 h).

4.2.7 Unit F: Alternating clay and sand with clay as lowermost deposit

High amplitude, high continuity reflections characterise the internal configuration of Unit F, with high order reflections between the main package boundaries comprising a low amplitude or acoustically transparent facies (Figs. 4.5; 4.6; 4.7). The unit stacks retrogradationally, the reflections onlapping Unit C (Fig. 4.7) or Unit D (Fig. 4.5). Alternatively, the reflections are erosionally truncated by the underlying surfaces of younger units (Fig. 4.6).

The unit forms a coast parallel, uniformly thick (~11 m) body of sediment, the position of which rests in the lee of Unit D (Fig. 4.2 e and f). Cores reveal the unit to be composed of clay with interbeds of sand (Fig. 4.8 g).

4.2.8 Unit G: Interbedded sand alternating with clay

Unit G is occurring in the most seaward extent of the study area, where it comprises landward and seaward dipping, moderate to high amplitude reflections that form a mounded geometry (Fig. 4.5) downlapping the top of Units E and F. The upper surface of the unit is often marked by pinnacles. The unit forms a narrow and discontinuous coast-parallel body that reaches up to 5 m in thickness (Fig. 4.2 f). The body comprises interbedded sands and clays.



Figure 4.8: Images of core samples from the study area. a) Quartz-rich pebble bearing sandstone with schist (Unit B). b) well-rounded cobbles with light grey to white clay (Unit C), c) gravel consisting of silcrete and quartz with sandstone (Unit B), d) sub to well-rounded pebble to cobbles with exotic clasts (Unit C), e) Pebbles with cemented shell hash. f) saprolite of sandstone and shale (Unit B), g) clay-rich sand (Unit F), h) pebbles (Unit E).

4.2.9 Unit H: Interbedded sand and mud alternating with sand and clay

Overlying Unit G, Unit H occurs as a cut and fill type reflection arrangement, with reflections draping the high points of Unit G and filling small channels (Fig. 4.7). Thin drapes of Unit H occur to landward of the high point created by Units C and D (Fig. 4.5). Reflections are typically concave up with alternating moderate to low amplitudes. The upper surface of the unit is truncated by WRS.

Thicknesses reflect the fill-like nature of the unit, with a series of disaggregated depocenters controlled by the underlying and undulating topography of Units G, C and D (Fig. 4.2 b, c and f). A maximum thickness of ~ 9 m occurs to the southeast where Unit G is absent (Fig. 4.2 f). Coring reveals these to comprise alternating muddy and sandy deposits.

4.2.10 Unit I: Clay

Unit I forms a thin (< 4m) clay-rich drape (Fig. 4.2 h) that covers the irregular surface of the gravels of Unit B and is constrained by highpoints in the bedrock basement (Fig. 4.5). The internal reflections alternate between high and low amplitudes and onlap the basement highs. The upper boundary of Unit I is WRS.

4.2.11 Unit J: Fine sand and mud

Forming the uppermost unit in the sedimentary package, Unit J overlies WRS and forms a dominantly acoustically transparent with occasional sub-horizontal, low amplitude backstepping reflections that onlap WRS increasingly landward and up dip. The unit spans the

entire study area, except where there is rocky outcrop in the nearshore areas (Fig 4.1). It reaches almost 15-thick in the south and thins to the north where bedrock crops out (Fig. 4.2j). The unit comprises fine sands and muds.

Table 4.1: Seismic unit description, thickness, internal reflector geometry, interpretation of depositional environment, lithology and age.

Unit	Underlying Unit	Description	Thickness (m)	Internal Reflector Geometry	Primary Lithology	Interpreted Age
Unit J	Units C, F, G, H, I	Uppermost sedimentary unit overlying the WRS. Thickens seaward in a wedge-like shape and spans the entire study area.	0 – 3.5 m	Dominantly acoustically transparent package with sub-horizontal, parallel to sub-parallel continuous reflectors that are seaward dipping. Low amplitude backstepping reflections that onlap WRS increasingly landward.	Soft Sediment – mud, fine sands	Late-Pleistocene to Holocene Transgression (MWP-1B)
Unit I	Units B, C, D, H	Relatively thin clay-rich unit that drapes over Unit B, C, D and H. Overlain by Unit J. relatively flat lying profile, also found between bedrock high points towards shore specifically overlying Unit B.	0 – 4.0 m	Variation between high and low amplitude internal configuration depending on underlying units and bedrock highs. Lacks internal configuration in some areas.	Clay	Plio-Pleistocene
Unit H	Units C, D, E, F, G	Highly variable in thickness as acts as a draping unit over undulating surfaces of Unit G in the west, and Units D and C landward. Thickness of infill is controlled by underlying undulating units. The upper surface is truncated by WRS.	0 – 9.0 m	A cut and fill type reflection arrangement. Medium to low amplitude reflector pattern, and reflections are typically concave up.	Interbedded sand and mud alternating with sand and clay	Plio-Pleistocene
Unit G	Units E and F	Most seaward unit forming a mounded geometry downlapping Units E and F. In the NW region it is more flat lying.	0 – 5.0 m	Comprises landward and seaward dipping moderate to high amplitude reflections clearly in the mounded feature. In the NW region the internal reflectors become more flat lying.	Interbedded sand alternating with clay.	Plio-Pleistocene

Unit F	Unit C, D and E	Unit stacking in aggrading and retrograding pattern on top of Unit E, while onlapping Unit C and D.	0 – 11.2 m	High amplitude, high continuity reflections (irregular, chaotic) with high order reflections between the main package boundaries comprising acoustically transparent facies.	Clay with interbeds of sand	Plio-Pleistocene
Unit E	PAB, Unit D	Prograding and aggrading unit overlying the PAB, onlapping Unit D. Forms the lower section of the barrier-spit features with an elevated undulatory surface and rugged erosional unconformity as the lower boundary with the basement.	0 – 6.0 m	Acoustically opaque throughout most of the study area. Medium to low amplitude internal reflectors; in some cases follow shape of unit (concave up).	Gravel (well-rounded pebbles with exotic clasts of jasper and agate)	Plio-Pleistocene Meso Gravel
Unit D	PAB, Unit C	Relatively flat lying aggrading and prograding unit in SE region with thin subfacies overlapping one another. Unconformably overlies Unit C in NW region in a flat lying to mounded profile. In SE region, onlaps Unit C in a wedge shape.	0 – 8.0 m	Sub-parallel and wavy seaward dipping prograding discontinuous internal reflectors. Chaotic and irregular in barrier-like features, concave up or down. Steep reflectors dipping seaward west of the mound, with shallow dipping reflection east going landward.	Sand	Plio-Pleistocene
Unit C	PAB, Unit B	Downlaps Unit B seaward. Largely undulating upper boundary. Varies in thickness with a variable shape from mound-like to relatively flatlying. Rugged lower boundary overlying basement.	0 – 8.9 m	Short, discontinuous reflectors, chaotic, irregular, no pattern. Bidirectional reflectors in the more flat lying shape.	Reworked gravel with light grey clay (well-rounded gravel with minor exotic clasts such as agate and jasper)	Plio-Pleistocene Proto Gravel
Unit B	PAB	Chaotic, rugged underlying surface. Mainly present	0 – 9.7 m	Low amplitude reflector pattern, sub-parallel,	Basal fining upward gravel	Early Eocene Proto gravel

		behind bedrock high points allowing deposition and partial shelter from erosion. Downlaps underlying unconformable SB1 surface and overlies basement prograding seaward, mound-like shape showing some aggradation.		wavy, relatively flatlying, chaotic and irregular in some cases. Represents a highly variable reflector configuration.	(well-rounded cobbles of sandstone and quartz-rich breccia with saprolite and shell)	
Offshore unit visible in mini airgun line (Fig. 4.3)	PAB	Extensive, thick, flat-lying unit, with elevated pinnacles moving further seaward	2.4 – 15.6 m	Undulatory, wavy, subparallel reflectors in the upper portion of the unit. Very low amplitude and semi-transparent reflector characteristic in central and lower portion of unit.	Formed through multiple sea level fluctuations and terrestrial aridification.	Oligocene to Pleistocene
*PAB (Unit A)		Land-attached high relief acoustic basement	Basement	Highly chaotic and rugged character at the basement surface, but reflectors dissipate with depth.	Metasedimentary basement	Proterozoic schist and Cretaceous siltstone

PAB – Proterozoic Acoustic Basement

Chapter 5: Discussion

The inner continental shelf stratigraphy offshore Mittag comprises several dispersed units of gravel, sand, mud and clay deposited onto an undulating bedrock topography. The stratigraphic architecture and lithological nature of these units provides insight into the genesis of submerged barrier spits and beaches, in addition to the controlling factors (allocyclic or autocyclic) responsible for their preservation.

5.1 SB1

The schist bedrock of the innermost shelf has undergone extensive erosion which has sculpted several terraces backed by small cliff lines (Fig. 4.4). Gradient knickpoints at approximately -78 msl, -65 msl and -55 msl occur and are the major autocyclic factor that controls available accommodation space in the shallow nearshore environment (Kirkpatrick et al., 2019). Where steps are present and backed by a cliff line, these provide preferential accommodation, shelter from transgressive ravinement processes, and a backstop against which shoreline materials can aggrade then prograde (Cooper et al., 2016; Cooper, Meireles, et al., 2018). Much of the context surrounding the distribution and nature of the sediments overlying SB1 are thus controlled by these antecedent conditions, as outlined below.

5.2 Gravel barrier and shoreline environments

5.2.1 Unit B

Overlying the acoustic basement and unconformably downlapping SB1, Unit B consists of two basal compositions. In the northern portion of the study area where the deposits are confined by bedrock pinnacles, Unit B consists of large, well-rounded cobbles of sandstone and quartz-rich breccia. To the south, with a less pronounced pinnacle-like bedrock morphology, the basal gravel comprises cobbles mixed with reworked pebbles of saprolite that fine up into sands with

increasing shelly content. Though less common on the southern Namibian shelf, saprolite has been documented in the north offshore Lüderitz, where it represents chemical weathering of the schist bedrock, potentially during the subaerial exposure of the Palaeocene (Green et al., 2024). Clast assemblages of the unit relate to the Proto-Orange River gravel suite which was delivered to the coast and inner shelf during the early to mid-Miocene (Nakashole et al., 2018). The reworked schist is believed to have been deposited directly from coarse bedload discharged from the Orange River (Spaggiari et al., 2006). Similar clast assemblages characterise the Plio-Pleistocene raised spits proximal to the Orange River mouth.

Unit B is interpreted as a set of disaggregated lag deposits concentrated along the shoreface via multiple phases of combined sea-level rise and fall. The lack of clear internal structure precludes an interpretation of the depositing environment, however its accumulation in bedrock lows points to reworking and preservation in localised areas of accommodation (Fig. 4.2 a). A similar layer directly overlying bedrock was described by Kirkpatrick et al. (2019) who ascribed it as multi-phase wave ravinement that produced a winnowed gravel lag spanning ages of Miocene to Pleistocene. The fining upward relates to post-transgressive settling to form a sand sheet (Goff et al., 2005).

5.2.2 Unit C

Unit C unconformably overlies the acoustic Neoproterozoic basement and downlaps Unit B with a basal elevation of -65 to -70 msl. The characteristic peaked or mounded shape and seaward and landward dipping reflections has been recognised on the shelf to the north by Runds et al. (2019), and to the south by Kirkpatrick et al. (2019). The authors interpreted these mounds as barrier spits. The seaward dipping reflections reflect foreshore deposition akin to the models described for onshore barrier-spit features (Spaggiari and Bordy, 2023). The

landward dipping reflections reflect the intertidal landward beach formed in the back barrier of the spit recurve (Fig. 5.1). The alternating clay and gravel internal layering of this landward beach represents washover materials advancing into the muddy backbarrier of the spit (Green et al., 2019).

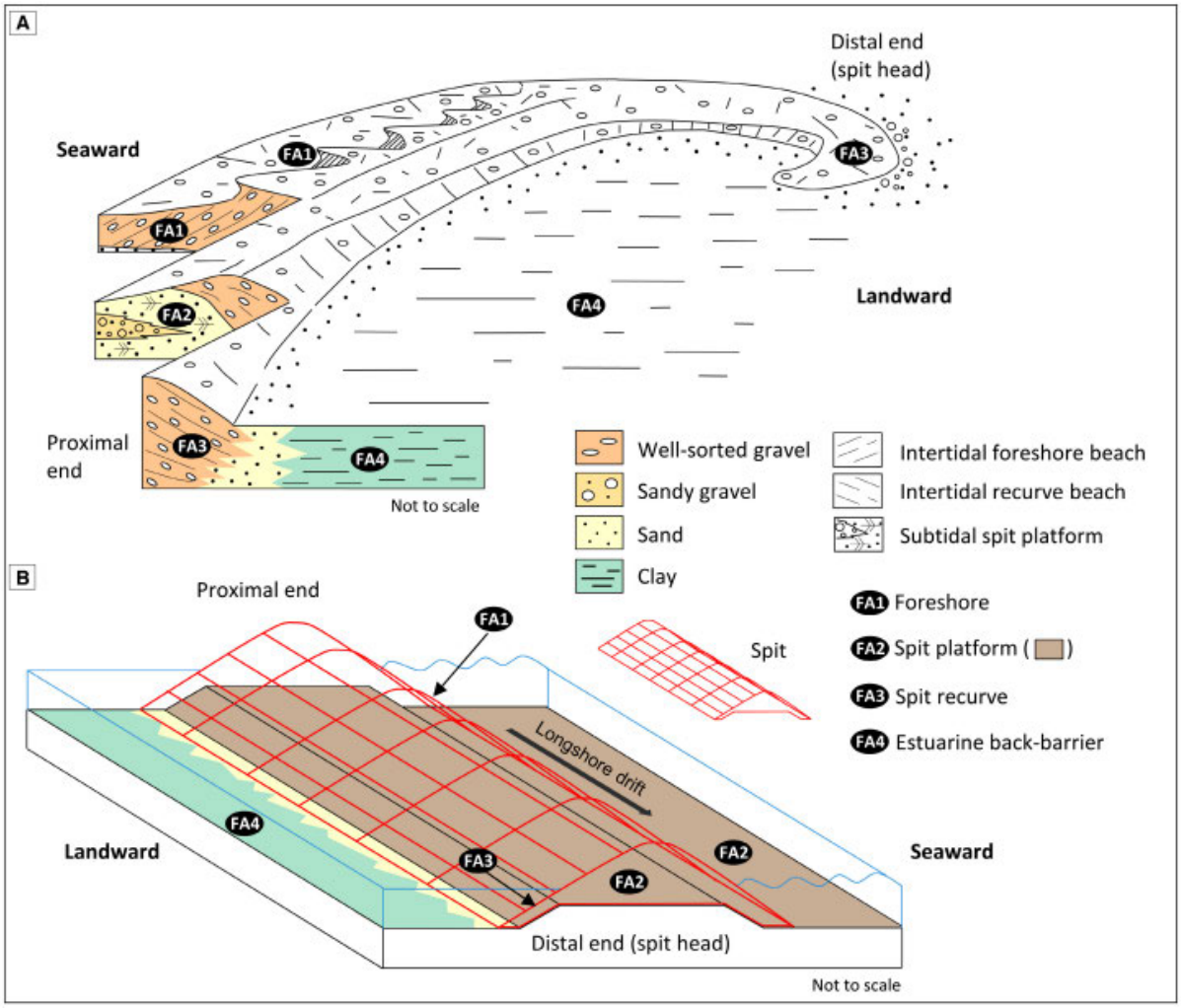


Figure 5.1: A conceptual model taken from Spaggiari and Bordy (2023) and modified from Spaggiari et al. (2006) to show the sedimentary architecture of a beach barrier complex and the different depositional environments. This model focuses on the formation of spit recurve and the sediments associated with a spit barrier.

Like Unit B, a similar clast assemblage indicates a Proto-Orange River gravel suite grouping and late Miocene delivery. Unit C appears to be a progradational to aggradational body derived from wave reworking of Unit B and foreshore accumulation to the spit body (Hine, 1979; Lindhorst et al., 2008; Robin et al., 2020). The aggradational component relates to a period of stillstand and normal regression of the body, forming a mound that prograded into both the

backbarrier and shoreface (Costas et al., 2006; Costas and FitzGerald, 2011; Tillmann and Wunderlich, 2013).

5.2.3 Unit D

The sandy and linear body of Unit D is associated with the flat portion of the bedrock surface between -60 m and -70 m. Like Unit C, it is characterised by a mounded shape, but with shallowly landward dipping to flat lying reflections that transition to seaward dipping varieties. The internal geometry is like the spit platform and foreshore of Spaggiari and Bordy's (2023) (Fig. 5.1) emergent spit examples, including a similar grain size and texture. The stacking arrangement between Unit C and D thus appears to be transgressive, with the foreshore resting further up-dip and landward. The most landward occurring examples (e.g. Fig. 4.6.) show that the spit platform has welded to the steepened bedrock profile at ~ 54 m depth.

5.2.4 Unit E

Unit E forms seaward of the -78 m change in bedrock gradient and comprises sand with mixed and well-rounded pebbles of jasper and agate, indicative of the Meso-Orange River gravels of the Plio-Pleistocene. Unit E forms a very linear body with poorly resolved internal reflections. The stacking pattern is not clear, though it onlaps the barrier spits of Unit C and D. It may comprise a mixed sand-gravel shoreface extension of the foreshore of these units (Frey and Dashtgard, 2011; Hart and Plint, 1989).

5.2.5 Unit G

Unit G marks a landward movement of the depositional locus (Fig. 4.2f). The bulk of material comprises sand, with minor clay components, and it forms a narrow and coast parallel, elongate body. Though no investigations on the internal structure of the sand spits offshore Walvis Bay

in Namibia have been undertaken, the general morphology is similar in terms of length, thickness and shape to that of Unit G (Fig. 5.2). The internal structure looks similar to the smaller sand spits that front the lagoons of SE Africa (Green et al., 2019) and it is on this basis that Unit G is interpreted as a sandy spit. Its base occurs at ~ 70 m depth and matches the barrier elevations observed by Runds et al. (2019) to the north.

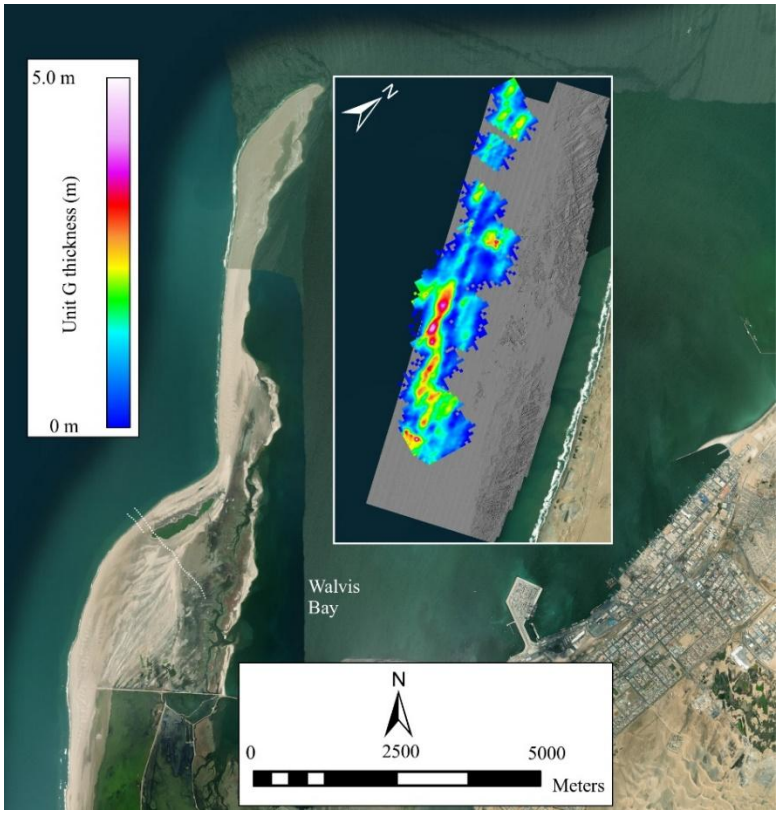


Figure 5.2: Comparison between the sand spit located offshore the Walvis Bay coast of Namibia, and the sandy spit morphology of Unit G.

5.3 Back barrier facies and environments

5.3.1 Unit F

The retrograding reflections comprising alternating clay and sand indicate a turnaround from a dominantly propagational system to a transgressive one. The landward dipping reflections look similar to the internal structure of washover fans from Ground Penetrating Radar (GPR) (Hein et al., 2014; Hein et al., 2016) and seismic reflection (Cooper et al., 2016), and their lithological character denotes frequent washover into a muddy back barrier.

5.3.2 Unit H and I

Unit H is made up of interbedded sand and mud alternating with sand and clay. It acts as an infilling unit as it accumulates and drapes over the high points of Unit G, as well as fills the crevices of the underlying gravel Unit C and Unit D. Due to the draping nature of the unit and varying thickness, it is suggested that Unit H is a back barrier deposit associated with the sandy spit of Unit G.

Unit I comprises a clay-rich drape that covers the undulating and irregular surface of the Unit B gravels between high points in the basement, onlaps the Unit E and F barrier systems, and drapes Unit H. It seems likely this is a similar back barrier accumulation, related to the most recent barrier spit to form (Unit G).

5.3.3 Wave ravinement surface (WRS) and post ravinement cover Unit J

WRS truncates all the stratigraphy, merging in places with the subaerial unconformity where the bedrock crops out at the seabed. The surface represents the final stage of erosion as wave bases translated landward during the deglaciation of the Pleistocene and Holocene. The overlying Unit J comprises clays, silts and fine sands (Kirkpatrick et al., 2019) and reflects the modern highstand materials forming the contemporary shoreface of the area. Unit J thickens to the southeast (Fig. 4.2 i), indicating shallower bedrock elevations in the northern portions of the study area with bedrock control lessening to the southeast.

5.4 The early shelf gravels: early to late Miocene pulses

The distribution of the beaches comprising the first gravel fluxes reflects the strong bedrock control on available accommodation for gravel accumulation. There is no clear depth constraint

to the beaches, and they reflect composite and reworked pockets of gravel with no discernible relationship to sea level. They are thus a function of autocyclic conditioning from the bedrock surface but concentrated by the allocyclic controls of the long-persisting and intense wave regime (Bluck et al., 2007).

The first gravel deposition played a role in later inheritance of the secondary pulses of gravel. The thickest pockets of material are backed by steeper topography, suggesting that the last phase of transgression in the late Miocene was responsible for the final pattern in gravel distribution of these early beaches. Unit C is almost entirely concentrated along the seaward edge of Unit B, where the steeper topography and seafloor roughness promoted swash bar welding and causes the progradation of the nascent barrier beach system to a palaeo-depth of ~ 65 m.

5.5 The next generation: Late Pliocene to Pleistocene/Holocene pulses

The anchoring of Unit D against steeper bedrock topography and the more landward high points made by Unit B prompted a spit platform to develop as accommodation to landward was filled and the spit began to prograde seaward with the influx of gravel materials at this stage. Unit D extended to a palaeo-depth of -70 m and the edge of the terrace in the bedrock surface. Unit E onlaps the front edge of Unit D and forms a narrow gravel ridge that marks a return to transgressive conditions.

5.6 Controls on beach emplacement and preservation

Tectono-eustatic fluctuations in sea-level occurred due to upliftment events in Cretaceous-Palaeocene and Middle Oligocene (Fig. 2.1). These periods of upliftment led to sea-level regression, subaerial exposure of the shelf, and the delivery of gravel to the coastline. Later

modifications, specifically during the rhythmic fluctuations of sea level during the Pleistocene have acted to create and preserve a series of barrier spit and back barrier environments on the shelf.

Runds et al. (2019) and Kirkpatrick et al. (2019) provided a series of models for the formation of gravel barriers at ~ 70-65 m below sea level, which they related to a prolonged slowstand at ~ 14.0 to 13.3 ka cal BP. This provided the impetus for strong wave reworking of the older gravel lags of Unit B to form a barrier-back barrier system. This was then preserved via overstepping of the barrier between 11.5 and 11.2 ka cal BP, associated with MWP-1B. It is not however clear how the regressive barrier systems fit within this model scheme, and pending the AMS 14C radiocarbon dates, the timing and genesis of these is unclear.

One of the overarching factors in the preservation of these features is the antecedent topographic control. Given the delivery of gravels throughout periods of hinterland uplift, in addition to the multiple forced regressions that would have been associated with the Pleistocene lowstands (Fig. 2.1), preservation potential along the inner shelf seems low. However, given the irregularities in the bedrock surface, erosion by subaerial processes may have been ameliorated in the sheltering lee of these irregularities. Further, during transgression, they provide a pinch point for aggradation, increasing barrier volume and thus the inertial constraints required to remove the barrier fully (Cooper et al., 2018b; Green, et al., 2018).

Figure 5.3 provides an evolutionary model for the inner shelf stratigraphy, focusing on the barrier features preserved in the stratigraphy.

a) Development of SB1. Creation of a broad sheltering lee in the bedrock profile.

b) Delivery of Pre-Proto and Proto Orange gravels, formation of Unit B lag from repeated regression and transgression. Unit B preserved in surface irregularities.

c) Normal regression produced a series of prograded barrier spits of Unit C with Meso-Orange River gravels.

d) Forced regression produced downstepping barriers of Unit D that were accommodated in a low-lying terrace in the bedrock surface.

e) Normal regression followed, producing aggradation and progradation of a mixed sand gravel shoreface, Unit E.

f) Development of sandy barrier Unit G which rolls over its former back barrier, Unit F. Unit H forms the new back barrier.

g) Aggradational growth of Unit G during slowstand causes back barrier flooding and impoundment associated with Unit G stability and growth ~14.0 to 13.3 ka cal BP. Unit I continues to flood landwards as an extensive back barrier lagoon develops.

h) The barrier and back barrier complex is overstepped by MWP-1B.

i) Transgression ensues, forming the wave ravinement surface and overlying high stand sediment wedge.

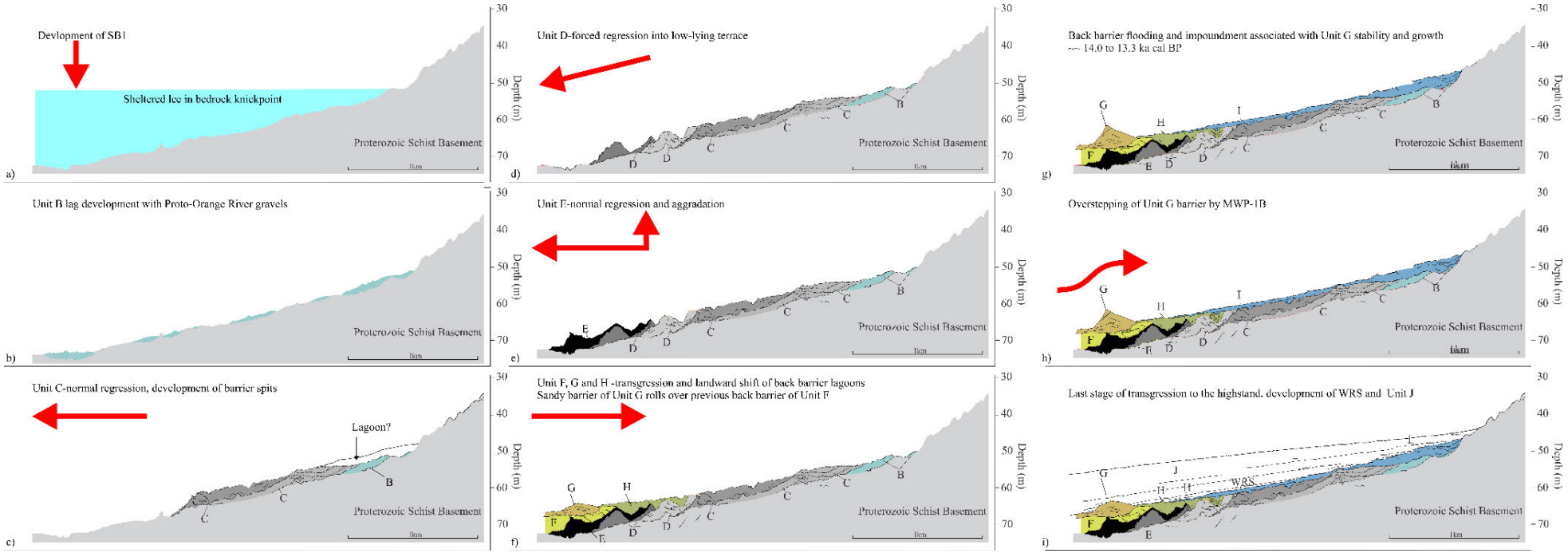


Figure 5.3: Evolutionary model showing the process of formation and subsequent preservation of the barrier features in the inner shelf stratigraphy.

Chapter 6: Conclusion

The evolutionary model for the inner shelf stratigraphy (Fig. 5.3), particularly the barrier features, demonstrates a complex interplay of geological processes. Initially, the development of SB1 created a broad sheltering lee in the bedrock profile. Subsequent deliveries of Pre-Proto and Proto Orange River gravels led to the formation of Unit B lag during repeated regressions and transgressions. Normal regression produced prograded barrier spits (Unit C) with Meso Orange River gravels, followed by forced regression that formed downstepping barriers (Unit D) on a low-lying terrace. Normal regression continued, resulting in the aggradation and progradation of a mixed sand-gravel shoreface and spit body (Unit E).

With the reduction in gravel load, a sandy barrier, Unit G, was created. Transgression resulted in this barrier rolling over its former back barrier (Unit F), forming a new back barrier (Unit H). Aggradational growth of Unit G during a slowstand preceding MWP-1B caused back barrier flooding (Unit I) impoundment, the development of a large barrier spit-lagoon system between ~14.0 to 13.3 ka cal BP. This was subsequently overstepped by MWP-1B (11.5 and 11.2 ka cal BP), aided by the long relaxation time of the gravels and the backing topography which added additional intertidal constraints in (re) moving the barrier systems.

The units deposited either formed in small slope irregularities in the bedrock surface or were impounded against topography created by preceding barrier spit development. Such a case emphasizes the important role that geological control plays in the development of barrier systems. The small irregularities further provide shelter from subaerial erosion, where small pockets of accommodation can exist despite forced regression (e.g. Unit B).

The rhythmic fluctuations of sea level during the Pleistocene have acted to create and preserve a series of barrier spit and back barrier environments on the shelf via normal regression and later overstepping of the barrier and back barrier complex. These barriers thus provide useful

means to track stepped rises in sea level and it is recommended that additional sampling and dating over the various deposits occur. This is however difficult given the polcyclic nature of the various gravels comprising each barrier, and the difficulty in identifying materials in life position within a gravel body.

References

Apollus, L., 1995. The distribution of diamonds on a late Cainozoic gravel beach, southwestern Namibia. University of Glasgow (United Kingdom).

Baby, G., Guillocheau, F., Morin, J., Ressouche, J., Robin, C., Broucke, O., Dall'Asta, M., 2018. Post-rift stratigraphic evolution of the Atlantic margin of Namibia and South Africa: Implications for the vertical movements of the margin and the uplift history of the South African Plateau. Marine and Petroleum Geology 97, 169-191.

Bluck, B., Ward, J., Cartwright, J., Swart, R., 2007. The Orange River, southern Africa: an extreme example of a wave-dominated sediment dispersal system in the South Atlantic Ocean. Journal of the Geological Society 164, 341-351.

Bluck, B.J., Ward, J.D., Spaggiari, R., 2001. Gravel beaches of southern Namibia. Ecology and geomorphology of coastal shingle, 56-76.

Braun, J., Beaumont, C., 1989. A physical explanation of the relation between flank uplifts and the breakup unconformity at rifted continental margins. Geology 17, 760-764.

Bremner, J., Willis, J., 1993. Mineralogy and geochemistry of the clay fraction of sediments from the Namibian continental margin and the adjacent hinterland. Marine Geology 115, 85-116.

Catuneanu, O., 2006. Principles of Sequence Stratigraphy. Elsevier, Alberta, Canada.

Compton, J.S., Bergh, E.W., 2016. Phosphorite deposits on the Namibian shelf. Marine Geology 380, 290-314.

Cooper, J., Green, A., Compton, J., 2018. Sea-level change in southern Africa since the Last Glacial Maximum. Quaternary Science Reviews 201, 303-318.

Cooper, J., Green, A., Meireles, R.P., Klein, A.H., Souza, J., Toldo, E.E., 2016. Sandy barrier overstepping and preservation linked to rapid sea level rise and geological setting. Marine Geology 382, 80-91.

Cooper, J., Meireles, R., Green, A., Klein, A.H., Toldo, E., 2018. Late Quaternary stratigraphic evolution of the inner continental shelf in response to sea-level change, Santa Catarina, Brazil. Marine Geology 397, 1-14.

Costas, S., Alejo, I., Rial, F., Lorenzo, H., Nombela, M.A., 2006. Cyclical evolution of a modern transgressive sand barrier in Northwestern Spain elucidated by GPR and aerial photos. Journal of Sedimentary Research 76, 1077-1092.

Costas, S., FitzGerald, D., 2011. Sedimentary architecture of a spit-end (Salisbury Beach, Massachusetts): The imprints of sea-level rise and inlet dynamics. Marine Geology 284, 203-216.

De Decker, R., 1988. The wave regime on the inner shelf south of the Orange River and its implications for sediment transport. South African Journal of Geology 91, 358-371.

De Vera, J., Granado, P., McClay, K., 2010. Structural evolution of the Orange Basin gravity-driven system, offshore Namibia. Marine and Petroleum Geology 27, 223-237.

Dingle, R., 1992. Structural and sedimentary development of the continental margin off southwestern Africa. Communications of the Geological Survey of Namibia 8, 35-43.

Dingle, R., Scrutton, R., 1974. Continental breakup and the development of post-Paleozoic sedimentary basins around southern Africa. Geological Society of America Bulletin 85, 1467-1474.

Fouché, J., Bate, K., Van der Merwe, R., 1992. Plate tectonic setting of the Mesozoic Basins, southern offshore, South Africa: A review, Conference on inversion tectonics of the Cape Fold Belt, pp. 33-45.

Frey, S.E., Dashtgard, S.E., 2011. Sedimentology, ichnology and hydrodynamics of strait-margin, sand and gravel beaches and shorefaces: Juan de Fuca Strait, British Columbia, Canada. Sedimentology 58, 1326-1346.

Garnett, R.H., 2017. Marine placer diamonds, with particular reference to Southern Africa., Handbook of marine mineral deposits. Routledge, pp. 103-142.

Garzanti, E., Andò, S., Limonta, M., Fielding, L., Najman, Y., 2018. Diagenetic control on mineralogical suites in sand, silt, and mud (Cenozoic Nile Delta): Implications for provenance reconstructions. Earth-Science Reviews 185, 122-139.

Goff, J.A., Austin Jr, J.A., Gulick, S., Nordfjord, S., Christensen, B., Sommerfield, C., Olson, H., Alexander, C., 2005. Recent and modern marine erosion on the New Jersey outer shelf. Marine Geology 216, 275-296.

Green, A.N., Pillay, T., Cooper, J.A.G., Guisado-Pintado, E., 2019. Overwash-dominated stratigraphy of barriers with intermittent inlets. Earth Surface Processes and Landforms 44, 2097-2111.

Green, A.N., Senna, W., Cooper, J., Heeralal, T., Labuschagne, H., 2024. Antecedent bedrock control on the sediment-starved continental shelf of south/central Namibia. Marine Geology, 107242.

Guillocheau, F., Rouby, D., Robin, C., Helm, C., Rolland, N., De Veslud, C.L.C., Braun, J., 2012. Quantification and causes of the terrigeneous sediment budget at the scale of a continental margin: a new method applied to the Namibia–South Africa margin. Basin Research 24, 3-30.

Hallam, C.D., 1964. The geology of the coastal diamond deposits of southern Africa (1959). The Geology of some Ore Deposits of Southern Africa. Geological Society of South Africa, Johannesburg., pp. 671-728.

Hart, B., Plint, A., 1989. Gravelly shoreface deposits: a comparison of modern and ancient facies sequences. Sedimentology 36, 551-557.

Hein, C.J., FitzGerald, D.M., de Menezes, J.T., Cleary, W.J., Klein, A.H., Albernaz, M.B., 2014. Coastal response to late-stage transgression and sea-level highstand. GSA Bulletin 126, 459-480.

Hein, C.J., FitzGerald, D.M., de Souza, L.H., Georgiou, I.Y., Buynevich, I.V., Klein, A.H.d.F., de Menezes, J.T., Cleary, W.J., Scolaro, T.L., 2016. Complex coastal change in response to autogenic basin infilling: An example from a sub-tropical Holocene strandplain. Sedimentology 63, 1362-1395.

Hine, A.C., 1979. Mechanisms of berm development and resulting beach growth along a barrier spit complex. Sedimentology 26, 333-351.

Hirsch, K.K., Scheck-Wenderoth, M., van Wees, J.-D., Kuhlmann, G., Paton, D.A., 2010. Tectonic subsidence history and thermal evolution of the Orange Basin. Marine and Petroleum Geology 27, 565-584.

Hoyt, J.H., Oostdam, B., Smith, D.D., 1969. Offshore sediments and valleys of the Orange river (South and South West Africa). Marine Geology 7, 69-84.

Jacob, J., 2001. Late Proterozoic bedrock geology and its influence on neogene littoral marine diamondiferous trapsites, MA1-Sperrgebiet, Namibia. University of Cape Town.

Jacob, J., Ward, J., Bluck, B., Scholz, R., Frimmel, H., 2006. Some observations on diamondiferous bedrock gully trapsites on Late Cainozoic, marine-cut platforms of the Sperrgebiet, Namibia. Ore Geology Reviews 28, 493-506.

Kirkpatrick, L., Green, A., 2021. Mapping diamondiferous palaeo-shorelines in complicated terrain: seismic and GIS-based methods from the inner shelf of southern Namibia. Geo-Marine Letters 41, 41.

Kirkpatrick, L.H., Green, A.N., 2018. Antecedent geologic control on nearshore morphological development: The wave dominated, high sediment supply shoreface of southern Namibia. Marine Geology 403, 34-47.

Kirkpatrick, L.H., Green, A.N., Pether, J., 2019. The seismic stratigraphy of the inner shelf of southern Namibia: the development of an unusual nearshore shelf stratigraphy. Marine Geology 408, 18-35.

Kuhlmann, G., Adams, S., Campher, C., van der Spuy, D., di Primio, R., Horsfield, B., 2010. Passive margin evolution and its controls on natural gas leakage in the southern Orange Basin, blocks 3/4, offshore South Africa. Marine and Petroleum Geology 27, 973-992.

Lancaster, N., Ollier, C., 1983. Sources of sand for the Namib sand sea. Zeitschrift für Geomorphology Supplement Band 45, 71-83.

Lindhorst, S., Betzler, C., Hass, H.C., 2008. The sedimentary architecture of a Holocene barrier spit (Sylt, German Bight): Swash-bar accretion and storm erosion. Sedimentary Geology 206, 1-16.

Lister, G., Etheridge, M., Symonds, P., 1991. Detachment models for the formation of passive continental margins. Tectonics 10, 1038-1064.

Lovecchio, J.P., Rohais, S., Joseph, P., Bolatti, N.D., Ramos, V.A., 2020. Mesozoic rifting evolution of SW Gondwana: a poly-phased, subduction-related, extensional history responsible for basin formation along the Argentinean Atlantic margin. Earth-Science Reviews 203, 103138.

Mitchum Jr, R.M., Vail, P.R., Sangree, J.B., 1977. Seismic stratigraphy and global changes of sea level: Part 6. Stratigraphic interpretation of seismic reflection patterns in depositional sequences: Section 2. Application of seismic reflection configuration to stratigraphic interpretation. AAPG Bulletin, 117-133.

Mitchum Jr, R.M., Vail, P. R., Thompson III, S. , 1977. Seismic stratigraphy and global changes of sea level: Part 2. The depositional sequence as a basic unit for stratigraphic analysis: Section 2. Application of seismic reflection configuration to stratigraphic interpretation. AAPG Bulletin, 53-62.

Murray, L.G., Joynt, R., O'Shea, D.O.c., Foster, R., Kleinjan, L., 1970. The geological environment of some diamond deposits off the coast of South West Africa. HM Stationery Office.

Nakashole, A.N., Hodgson, D.M., Chapman, R.J., Morgan, D.J., Jacob, R.J., 2018. Long-term controls on continental-scale bedrock river terrace deposition from integrated clast and heavy mineral assemblage analysis: An example from the lower Orange River, Namibia. Sedimentary Geology 364, 103-120.

Rabinowitz, P.D., LaBrecque, J., 1979. The Mesozoic South Atlantic Ocean and evolution of its continental margins. Journal of Geophysical Research: Solid Earth 84, 5973-6002.

Robin, N., Levoy, F., Anthony, E.J., Monfort, O., 2020. Sand spit dynamics in a large tidal-range environment: Insight from multiple LiDAR, UAV and hydrodynamic measurements on multiple spit hook development, breaching, reconstruction, and shoreline changes. Earth Surface Processes and Landforms 45, 2706-2726.

Rogers, J., 1977. Sedimentation on the continental margin off the Orange River and the Namib Desert., Department of Geological Sciences. University of Cape Town.

Rogers, J., Rau, A., 2006. Surficial sediments of the wave-dominated Orange River Delta and the adjacent continental margin off south-western Africa. African Journal of Marine Science 28, 511-524.

Roksandić, M., 1978. Seismic facies analysis concepts. Geophysical prospecting 26, 383-398.

Runds, M.J., 2018. Sedimentology and depositional environment of a marine target, Southern Namibia: 3D stratigraphic architecture and diamond mineralisation potential., Department of Geological Sciences. University of Cape Town.

Runds, M.J., Bordy, E.M., Pether, J., 2019. Late Quaternary sedimentological history of a submerged gravel barrier beach complex, southern Namibia. Geo-Marine Letters 39, 469-491.

Sheriff, R., 1976. Inferring stratigraphy from seismic data. AAPG Bulletin 60, 528-542.

Spaggiari, R., Bluck, B., Ward, J., 2006. Characteristics of diamondiferous Plio-Pleistocene littoral deposits within the palaeo-Orange River mouth, Namibia. Ore Geology Reviews 28, 475-492.

Spaggiari, R., Bordy, E.M., 2023. Anatomy of a diamondiferous gravel barrier spit at the palaeo-Orange River mouth, south-western Namibia. Sedimentology 70, 1630-1654.

Stevenson, I., McMillan, I., 2004. Incised valley fill stratigraphy of the Upper Cretaceous succession, proximal Orange Basin, Atlantic margin of southern Africa. Journal of the Geological Society 161, 185-208.

Tillmann, T., Wunderlich, J., 2013. Barrier rollover and spit accretion due to the combined action of storm surge induced washover events and progradation: Insights from ground-penetrating radar surveys and sedimentological data. Journal of Coastal Research, 600-605.

Tucker, M.E., 1988. Techniques in sedimentology. Blackwell Scientific Publications.

Veeken, P., Van Moerkerken, B., 2013. Seismic stratigraphic techniques. EAGE and Elsevier Scientific Publishers.

Xu, G., Haq, B.U., 2022. Seismic facies analysis: Past, present and future. Earth-Science Reviews 224, 103876.